2017-12

Inhibition of aluminium corrosion using carica papaya extracts in acidic media (sulphuric acid and phosphoric acid)

Kasuga, Baruku

NM-AIST

https://doi.org/10.58694/20.500.12479/223

INHIBITION OF ALUMINIUM CORROSION USING *Carica papaya* EXTRACTS IN ACIDIC MEDIA (SULPHURIC ACID AND PHOSPHORIC ACID)

Baruku Zakaria Kasuga

A Dissertation Submitted in Partial Fulfilment of the Requirements for the Degree of Master's in Materials Science and Engineering of the Nelson Mandela African Institution of Science and Technology

Arusha, Tanzania

December, 2017

ABSTRACT

Corrosion inhibition of aluminium using *Carica papaya* leaves extracts in 1M H_2SO_4 and IM H_3PO_4 was investigated under different temperatures (30, 40 and 50^0C) and concentrations (from 20-100 v/v %). The inhibitor was found to work by being adsorbed onto the aluminium surface, hence preventing the corrosion of the metal by forming a film that acted like a barrier to the direct contact between the metal and the acids. Gravimetric analysis (Weight loss method) as the main methodology was used throughout the investigation. From the data collected, inhibition efficiency values, adsorption isotherms, kinetic and thermodynamic parameters concerning the adsorption processes were determined; all of these give out important clues on the working ability of the inhibitor. Characterization was also applied using Scanning Electron Microscope (SEM) and Fourier Transform Infrared (FT-IR) spectroscopy. SEM was used to determine the adsorption ability of inhibitor by investigating aluminium coupons through surface profile analysis. The FT-IR machine was used to determine functional groups of the phytochemicals found in *C. papaya* leaves, inhibitor prepared and those participated in adsorption. *Carica papaya* leaves extract was found to have a maximum inhibition efficiency of 71.67 % and 56.02 % in H_2SO_4 and H_3PO_4 respectively, at the optimal concentration which ranges from 60 to 80 v/v % in both of the media used. Results obtained in this study give hope to corrosion engineers that *C. papaya* is among of the plants on which its extracts can be used to develop a commercialized natural corrosion inhibitor. This is possible because it has phytochemicals with active functional groups to develop inhibitive properties.

DECLARATION

I, **Baruku Zakaria Kasuga** do hereby declare to the Senate of Nelson Mandela African Institution of Science and Technology that this dissertation is my own original work and that it has neither been submitted nor being concurrently submitted for degree award in any other institution.

Baruku Zakaria Kasuga

_____ _____

Name and signature of candidate **Date**

The above declaration is confirmed by

Dr. Revocatus Machunda

_____ _____

Name and signature of supervisor 1 **Date**

Prof. Eugene Park

_____ _____

Name and signature of supervisor 2 **Date**

COPYRIGHT

CERTIFICATION

This is to certify that the dissertation entitled **"*Inhibition of Aluminium corrosion using Carica papaya extracts in acidic media*"** submitted in partial fulfillment of the requirements for the award of a Master's degree in Materials Science and Engineering at Nelson Mandela African Institution of Science and Technology, Tanzania is an authentic work carried out by him under our mentorship.

_____ _____

Dr. Revocatus Machunda **Date**

(Supervisor 1)

_____ _____

Prof. Eugene Park **Date**

(Supervisor 2)

ACKNOWLEDGEMENTS

I particularly wish to express my sincere thanks and deep gratitude to my supervisors, Prof. Eugene Park and Dr. Revocatus Machunda for their efforts and support to make my research work successful.

I would like to extend my thanks and happiness to all other lecturers and classmates for their contributions and courage during all the time of my studies and accomplishment of this work. Finally, my appreciation goes to my parents and family for the constant support and encouragement.

DEDICATION

This piece of work is dedicated to my dearest parents, all my lecturers, and friends.

TABLE OF CONTENTS

LIST OF TABLES

LIST OF FIGURES

LIST OF ABBREVIATIONS

AFM : Atomic Force Microscope

CR : Corrosion rate

EDS : Energy Dispersive Spectroscopy

EIS : Electrochemical Impedance Spectroscopy

E_a : Activation energy

FT-IR : Fourier Transform Infrared Spectroscopy

GDP : Gross Domestic Product

SCE : Saturated calomel electrode

SEM : Scanning Electron Microscope

% IE : Percentage of inhibition efficiency

ΔG^0 : Standard Gibbs free energy of adsorption

ΔH_a^o : Enthalpy of activation

ΔQ_{ads} : Enthalpy of adsorption

ΔS^0 : Standard entropy of adsorption

v/v % : Concentration of volume by volume percentage

LIST OF APPENDICES

CHAPTER ONE

INTRODUCTION

This Chapter describes the general introduction of the study. It mainly focuses on the background information of the study, the problem statement, objectives, research questions, significance of the research and the general literature review.

1.1 Background information

Corrosion is an electrochemical process that involves the deterioration of material when subjected to an environment that can support it (Ayeni *et al.*, 2012). In developed countries, the cost of managing corrosion is approximately 5% of their Gross Domestic Product (GDP) (Schmitt, 2009). For developing countries like Tanzania, the annual cost of corrosion control is unknown. Measures to control corrosion must be taken since the economy of Tanzania is advancing leading to more use of materials in infrastructure projects.

To protect aluminium and its alloys from corrosion, various methods have been employed such as chromating, cathodic protection, organic coating and use of inhibitors (Mahendru Sr and Mahindru, 2011; Musa, 2012a). In various systems or material, corrosion inhibitors have been employed for a long time as one of the most applicable approaches with good results. Corrosion inhibitors are materials which when added in small amount to the environment under corrosion, effectively slow down its occurrence (Kesavan *et al.*, 2012). They can be classified into three types which are the organic, inorganic and mixed type (Aballe *et al.*, 2001; Ebenso *et al.*, 2008; Raja and Sethuraman, 2008; Umoren, 2009; Kesavan *et al.*, 2012; Rajendran *et al.*, 2012). These inhibitors have been found useful in industrial system and commercial application such as in cooling systems, refinery units, chemicals, oil and gas production units, boilers (Singh *et al.*, 2012). Due to the toxicity of synthetic corrosion inhibitors such as chromates, phosphate, and arsenic; recently, naturally occurring substances of plant extracts which are readily available, cheap, renewable, and eco-friendly have been successfully used as a replacement for synthetic corrosion inhibitors (Kesavan *et al.*, 2012).

Aluminium is one of the most abundant elements with wide applications. This is due to its attractive properties such as low density, good thermal and electrical conductivity. It has the ability to form a protective layer under a corrosive medium, however, it corrodes under highly acidic and alkaline media by dissolving of its oxide protective layer (El Maghraby,

2009; Loto, 2012). The current study is based on investigating the working ability of *Carica papaya* leaves extracts in developing inhibitive properties on the aluminium, found under acidic media.

1.1.1 Corrosion that attacks aluminium and its alloys

Below are the types of corrosion that attack aluminium and its alloys:

(i) General dissolution

General dissolution is a type of corrosion which attacks aluminium when found in highly acidic and alkaline environment. It can also involve lower alcohols, phenols and aqueous systems at high temperatures above 90^0C (Mahendru Sr and Mahindru, 2011).

(ii) Pitting

Pitting is a type of highly localized corrosion which occurs under aggressive chloride ions. The chlorides attack weak sites of the oxide and then propagate. The reaction proceeds by the evolution of hydrogen and reduction of oxygen as follows.

$$Al \rightarrow Al^{3} + +3e^{-} \quad (1)$$

$$Al^{3+} + 3H_2O \rightarrow Al(OH)_3 + 3H^{+} \quad (2)$$

$$2H^{+} + 2e \rightarrow H_2 \quad (3)$$

$$O_2 + 2H_2O + 4e \rightarrow 4OH \quad (4)$$

Reaction 1 and 2 produce positive charges which balance with negative charges by combining with Chloride ions to form HCl which deepens the pit. Due to reduction reaction, there is alkalinisation around particles at the cathode. This environment favours dissolution of aluminium oxide at that site to cause alkaline pits (Mahedru Sr and Mahindru, 2011; Musa, 2012b; Son *et al*., 2012).

(iii) Intercrystalline corrosion

Intercrystalline corrosion is a type of corrosion which occurs by dissolution of the grain boundary zone when the bulk remains intact. It is electrochemical because it involves micro galvanic cells formed due to the heterogeneity in alloy composition (Mahedru Sr and Mahindru, 2011).

(iv) Stress corrosion cracking

Stress corrosion cracking is a form of intergranullar corrosion which is starting with a stress from an environment that induces crack initiation and propagation along grain boundaries. Metallurgical, environmental and mechanical factors are associated with its occurrence. The areas along grain boundaries become anodic which make corrosion to propagate along them. It mostly affects aluminium alloys with a high amount of soluble alloying elements such as magnesium, copper, zinc, and silicon (Mahedru Sr and Mahindru, 2011; Musa, 2012b; Nakano *et al.*, 2012).

(v) Galvanic corrosion

Galvanic corrosion is a type of corrosion that occurs when dissimilar metals come into contact which causes electrical potential differences. The electrolytic condition also is necessary for the corrosion to occur because it forms a closed circuit. Aluminium corrode because it is more anodic than many of the other structural materials (Mahendru Sr and Mahindru, 2011; Musa, 2012b; Musa *et al.*, 2011).

1.1.2 Electrochemistry of aluminium corrosion in acidic medium

Although aluminum has a tendency to form a protective oxide layer against corrosion, in highly acidic or alkaline medium the layer can dissolve to allow the metal dissolution which favours its corrosion.

The following equations explain its occurrence in acidic medium (Hassan and Zaafarany, 2013).

Sulfuric acid (H_2SO_4)

$$Al_{(s)} \leftrightarrow Al^{3+} + 3e^{-} \; oxidation\,(anodic\ reaction) \qquad 5$$

$$2H^{+} + 2e \leftrightarrow H_{2(g)} reduction \ (cathodic\ reaction)$$ 6

Overall reaction

$$2Al_{(s)} + 6H_{(aq)}^{+} \leftrightarrow 2Al_{(aq)}^{3+} + 3H_{(g)} \quad (7)$$

From the equations above, the anodic reaction which is the dissolution of aluminum produces electrons which are picked into the cathodic site. These electrons cause the combination of the two $H_{Chemisorbed}$ on the metal surface to form H_2 molecules which come out as bubbles (Prabhu, 2013).

Phosphoric acid (H_3PO_4)

Aluminium dissolution by oxidation (anodic reaction) occurs as follows

$$Al + H_2O \rightarrow AlOH_{(ads)} + H^{+} + e^{-} \quad (8)$$

$$AlOH_{(ads)} + 5H_2O + H^{+} \rightarrow Al^{3+} + 6H_2O + 2e^{-} \quad (9)$$

$$Al^{3+} + H_2O \rightarrow [AlOH]^{2+} + H^{+} \quad (10)$$

Hydrogen gas formation by reduction (cathodic reaction) occurs as follows

$$H^{+} + e^{-} \rightarrow H_{(ads)} \quad (11)$$

$$H_{(ads)} + H_{(ads)} \rightarrow H_2 \quad (12)$$

(Prabhu, 2013).

Both of the reactions in sulphuric and phosphoric acid occur in the same way by oxidation of aluminium and reduction of hydrogen ions to form hydrogen gas, whereby the rate of gas production can be used to measure the corrosion rate.

In industrial applications involve aluminium; the contamination of it with aggressive media of either alkalinity or acidity may occur. For example, in aluminium pickling and cleaning, the green inhibitors have been used to prevent it from unexpected contamination (Kini *et al.*, 2011). But also aluminum used in the construction of water cooling systems, boilers and radiators can undergo corrosion, and green inhibitors have been used for protection (Laouali and Bénière, 2012; Kavitha *et al.*, 2014).

1.1.3 Corrosion inhibitors and their mechanism

Investigations show organic inhibitors, as well as green inhibitors, act by being adsorbed on the metal surface and form a barrier which protects it to become attacked by a corrosive medium. The adsorption can either be a chemical adsorption (chemisorption) (Ansari *et al.*, 2013; Dariva and Galio, 2014) or physical adsorption, which involves electrostatic attraction between the inhibitor and the metal surface (Abd-El-Nabey *et al.*, 2012). The protective film formed due to adsorption can be understood in detail by the use of FT-IR machine which identifies functional groups within it; therefore provide information about their participation. Other mechanisms may include increasing or decreasing of the anodic and/or cathodic reaction, decreasing the diffusion rate for the reactants to the surface of the metal or decreasing the electrical resistance of the metal surface (Rani and Basu, 2011).

1.1.4 Plants extract with halides

Due to low inhibition efficiencies of some plants' extracts, efforts on raising their efficiencies have been done by applying synergism, which involves a combination of the inhibitor with another, with a compound or an element. The following are some of the studies reported on synergism; (Umoren, 2009; Obot *et al*., 2011). The increase in inhibition efficiency when using halides is because they influence the adsorption power of some organic compounds found in plants' extracts.

1.1.5 Corrosion inhibition by *Carica papaya*

Carica papaya has been reported to contain alkaloids, flavanols, tannins, resin, benzylglucosinolate, saponins, papain, malic acid, methyl salicylate and anthraquinones, which are believed to be the cause of its inhibition property (Loto, 2012; Kavitha *et al.*, 2014). Studies concern *Carica papaya* as a corrosion inhibitor in sulfuric acid to the mild steel was observed to be caused by physical adsorption. Inhibition efficiency was found to

decrease with an increase in temperature and increase with an increase in concentration. All plant parts were examined and inhibition efficiency was found to have the following trend, leaves (93.88 %) > seeds (84.53%) > heartwood (71.49 %) > bark (54.59 %) at 303K. The experiments were conducted by using the weight loss method (Okafor, and Ebenso, 2007).

Synergistic effects of *C. papaya* leaves extract with Zn^{2+} in corrosion inhibition of mild steel in an aqueous medium with maximum efficiency of 91% have been reported. The optimal concentration was 2ml of CPL with Zn^{2+} (50 ppm) in 100 mL aqueous medium contains 60ppm of Cl^- ions. The study was simulated to work in water cooling system (Kavitha *et al.*, 2014). Through FT-IR machine, the complex combination of the extract with Zn^{2+} was found to be adsorbed on the metal surface as a coat. These results give hope of synergism to inhibition efficiency using halides under highly acidic or basic medium. Generally, inhibition efficiency of inhibitors mixed with halides has been reported to follow a trend of I >Br > Cl (Umoren, 2009). Other studies on *Carica papaya* leaves extracts involves inhibition of mild steel corrosion in nitric acid with an efficiency of 92.8 % and inhibition of duplex (α β) brass using the extracts of *C. Papaya* and *Camellia Sinensis* leaves in nitric acid with an efficiency of 68.97 %.

1.1.6 Methodology and experimental parameters

Different methodologies and experimental parameters are normally used in corrosion inhibition studies. The parameters measured are useful in the determination of inhibition efficiency, thermodynamic and kinetic parameters and adsorption isotherms involved.

(i) Weight loss measurement

The metal coupons, for instance aluminium coupons are immersed in the aggressive solution with inhibitor at different temperatures and concentrations. Then coupons are removed at a certain interval of time, followed by being washed and dried in a desiccator to cool at ambient temperature, and lastly weighed. The weight loss of the coupons in grams is used to calculate inhibition efficiency and the degree of surface coverage of inhibitor together with the corrosion rate of the metal (Avwiri and Igho, 2003; Amin *et al.*, 2009a; Obot and Obi-Egbedi, 2010).

(ii) Electrochemical measurements

Three electrode cells, platinum wire as a counter, saturated calomel electrode (SCE) as a reference and aluminium sheet-specimen as a working electrode is used. Potentiostat together with a computer with graphing and analysing software is used to provide the data. Data can be collected in two ways, potentiodynamic test and Electrochemical Impedance Spectroscopy (EIS).

Potentiodynamic test (Linear polarization measurements)

Electrochemical parameters measured here are the I_{corr} = corrosion current, E_{corr} = corrosion potential and Tafel slopes (Rajalakshmi *et al.,* 2010; Hamdy and El-Gendy, 2013; Shivakumar and Mohana, 2013).

Electrochemical Impedance Spectroscopy (EIS)

EIS measurements are taken by using alternating current signal. *Ny Quist* plots obtained from a connected computer are used to calculate double layer capacitance (C_{dl}) and Charge transfer resistance (R_t) which are the parameters in EIS (Hamdy *et al.*, 2006; Yurt *et al.*, 2006; Lebrini *et al.,* 2013).

1.1.7 Characterization of inhibitor and the adsorbed film

This is done to study constituents of inhibitor and the protective film formed after adsorption, where equipments such as Fourier Transform Infrared (FTIR) spectroscopy and Energy Dispersive Spectroscopy (EDS) have been used. The surface profile analysis of the metal under corrosion is mostly done by using equipment such as Scanning Electron Microscope (SEM) and Atomic Force Microscope (AFM) (Sangeetha *et al.,* 2011; Xiong *et al.*, 2013; Yadav *et al.*, 2015). This is done to confirm the formation of the adsorbed film.

1.1.8 Thermodynamic, kinetic parameters and adsorption isotherms

(i) Kinetic parameter (Activation energy)

The decrease in apparent activation energy in the presence of inhibitor normally denotes chemical adsorption while the reverse is usually attributed to physical adsorption (Ansari *et al.*, 2013; Yiase *et al.*, 2014). The higher activation energy implies the slow dissolution of metal.

(ii) Thermodynamic parameters

Enthalpy and entropy of activation, heat and Gibbs energy of adsorption are thermodynamic parameters which can be employed in the study of corrosion of metals (Ansari *et al.*, 2013; Yiase *et al.*, 2014). All of these parameters are calculated after collection of data, the positive values of enthalpy of activation reflects the endothermic nature of the metal dissolution and the negative values in the opposite way. The negative value of the Gibbs energy of adsorption implies spontaneity and stability of the inhibitor adsorption on the metal surface (Yiase *et al.*, 2014).

(iii) Adsorption parameters

The adsorption process of organic substances involves two types of the possible interaction termed as physical and chemical adsorption with the metal surface (Kesavan *et al.*, 2012; Yiase *et al.*, 2014). The adsorption isotherms provide important clues regarding the nature of the metal and inhibitor interaction. In order to determine the adsorption isotherm obeyed by the adsorption process, various adsorption isotherms such as Frumkin, Temkin, Freundlich and Langmuir are tested and the one with a high correlation coefficient is preferred (Abd-El-Nabey *et al.*, 2012).

1.2 Statement of the problem

Due to the toxicity of synthetic corrosion inhibitors, green corrosion inhibitors have been investigated and used nowadays. Plant extracts as natural and green inhibitors have been observed to contain active constituents (phytochemicals) to inhibit the corrosion of metals (Singh *et al.*, 2012). Several studies have been done on investigating *C. papaya* as a green inhibitor with promising results. Investigations on corrosion inhibition of mild steel with various efficiencies have been reported including, sulphuric acid (93.88% efficient), aqueous media (91% efficient) and Nitric acid (92.8% efficient) (Okafor and Ebenso, 2007; Loto *et al.*, 2011; Oki *et al.*, 2015).

Searching more about the conditions where *C. papaya* extracts can work much better is still of great importance, but investigation of it in corrosion inhibition of aluminium is not well documented. Investigation of the leaves' extracts constituents which have been participating in corrosion inhibition of aluminium and the working ability of the extracts at various temperatures, as well as thermodynamic and kinetic parameters are not well reported. The

current study dealt with the inhibition of aluminium corrosion using *Carica papaya* leaves extracts in acidic media. In general investigations of natural materials on their ability to inhibit corrosion broaden a foundation on designing and developing green inhibitors to the corrosion engineers.

1.3 Research objectives

1.3.1 General objective

Evaluation of the corrosion inhibition of *Carica papaya* extracts on the aluminium metal in acidic media.

1.3.2 Specific objectives

i) Determination of kinetic, thermodynamic parameters and adsorption isotherms of *C. papaya* extract on aluminum corrosion under H_2SO_4
ii) Determination of kinetic, thermodynamic parameters and adsorption isotherms of *C. papaya* extract on aluminum corrosion under H_3PO_4

1.3.3 Research questions

i) What are the kinetic, thermodynamic parameters and adsorption isotherms of *C. papaya* extract on aluminum corrosion under H_2SO_4?
ii) What are the kinetic, thermodynamic parameters and adsorption isotherms of *C. papaya* extracts on aluminum corrosion under H_3PO_4?

1.4 Significance of the study

Detail information on inhibition of aluminium corrosion by the use *Carica papaya* extracts is going to be obtained which is very important for the corrosion engineers/applicants of corrosion inhibitors, especially in industries. There is also a high expectation of developing an eco-friendly inhibitor with much availability since pawpaw plants are widely grown in Tanzania.

CHAPTER TWO

INHIBITION OF ALUMINIUM CORROSION USING *Carica Papaya* LEAVES EXTRACT IN SULPHURIC ACID[1]

Abstract

Inhibition of aluminium corrosion using *C. papaya* leaves extract in 1.0 M H_2SO_4 was investigated by using gravimetric analysis at various concentrations and temperatures: 303 K, 313 K and 323 K. Characterization was done by using Scanning Electron Microscope (SEM) and Fourier Transform Infrared (FT-IR) spectroscopy. Results show that inhibiting ability of the extract was due to its adsorption onto the metal surface through Langmuir adsorption isotherm. Thermodynamic (Gibbs energy, entropy and heats of adsorption) and kinetic parameters (activation energy and entropy of activation) were also determined. All of these agreed to physical adsorption of inhibitor onto the aluminium surface.

Keywords: *C. papaya*, inhibition, aluminium, sulphuric acid, adsorption, thermodynamic and kinetic parameters

[1] Journal of Minerals and Materials Characterization and Engineering , 2018**: 6** 1-14

2.1 Introduction

Although aluminium is thermodynamically reactive, it is the only metal with a property of protecting itself against corrosion by forming an amphoteric oxide film, which protects it against further attack when found under aggressive medium. In a highly aggressive medium, of either alkalinity (pH> 9) or acidity (pH< 5), aluminium and its alloys corrodes by dissolving of its protective oxide layer (Oguzie, 2007; Li and Deng, 2012). Various industrial applications may cause aluminium to come into contact with aggressive media. Some of them include pickling, anodizing (surface treatments) and metal cleaning/ descaling which involves the use of H_2SO_4, HCl, H_3PO_4 and other acids. To overcome such situation corrosion inhibitor must be introduced to control and rescue the metal from being attacked (Moutarlier *et al.*, 2005; Zaferani *et al.*, 2013).

The interest of investigating plants' extracts as corrosion inhibitors is increasing nowadays due to the fact that, synthetic (inorganic) corrosion inhibitors such as chromates, phosphates, and molybdates have some kind of toxicity. Researches show that plants' extracts are rich in phytochemicals with heteroatoms such as S, O, and N which makes them active in developing inhibitive properties (Rani and Basu, 2011). Also, it has been reported especially for those with S and N are suitable in acids (Quraishi *et al.*, 2010).

Various plants' extracts have been investigated and show good inhibitive ability. *C. papaya* has been reported several times to have a wide spectrum of phytochemicals which among of them are corrosion inhibitive. Some of the reported findings involve, *C. papaya* extracts on the corrosion of mild steel (Okafor and Ebenso, 2007), inhibition effect of extracts of *C. papaya* and *Camellia sinensis* leaves (Loto *et al.*, 2011), electrochemical corrosion behaviour of mild steel reinforced concrete in H_2SO_4 (Loto, 2012), performance of mild steel in nitric acid/*C. papaya* leaf extracts corrosion (Oki *et al.*, 2015) and synergistic effects of *C. papaya* leaves extract with Zn^{2+} in corrosion inhibition of mild steel in aqueous medium (Kavitha *et al.*, 2014). In the current study, *C. papaya* has been investigated as a corrosion inhibitor of aluminium in 1.0 M H_2SO_4. Gravimetric analysis (Weight loss method) employed in this study is associated with, inhibition efficiency, the degree of surface coverage and corrosion rate as follows:

Inhibition efficiency (%), $$I.E = \left(1 - \frac{W_{inh}}{W_{blank}}\right) \times 100 \qquad (13)$$

Degree of surface coverage,

$$\theta = \left(1 - \frac{W_{inh}}{W_{blank}}\right) \quad (14)$$

Where, % IE= Inhibition efficiency, W_{inh}= Weight loss in presence of inhibitor, W_{blank}= Weight loss in absence of inhibitor and θ = Surface coverage of inhibitor (Umoren *et al*., 2009; Nwosu *et al*., 2014).

The corrosion rate using the formula

$$CR\left(gcm^{-2}h^{-1}\right) = \frac{W}{At} \quad (15)$$

Where; CR= Corrosion rate, A= Coupons surface area (cm^2), t = immersion time in hours W = Weight loss (Obi-Egbedi *et al.*, 2012; Eddy *et al.*, 2015).

In case of Activation energy values; Equation below is used

$$lnCR = \left(\frac{-E_a}{RT}\right) + lnA \quad (16)$$

Where, $\ln CR versus \frac{1}{T}$ is a straight line with a slope of $-\frac{E_a}{R}$ which is used to calculate the activation energies (Nahlé *et al*., 2012; Obi-Egbedi *et al*., 2012).

Enthalpies of Activation values are obtained by plotting the graph of $\ln\frac{CR}{T} versus \frac{1}{T}$, for each temperature. $-\frac{\Delta H^0}{R}$ values as slopes are used to calculate enthalpies of activation and $\ln\left(\frac{R}{Nh}\right) + \frac{\Delta S^0}{R}$ as intercepts to calculate the entropy values. Below is the equation used

$$CR = \frac{RT}{Nh}\exp\left(\frac{\Delta S_a^o}{R}\right)\exp\left(-\frac{\Delta H_a^o}{RT}\right) \quad (17)$$

Where h is the plank's constant 6.626176 x 10^{34}, N is Avogadro's number 6.02252 x 10^{23} mol^{-1}

ΔS_a^o *is the entropy of activation and* ΔH_a^o *is enthalpy of activation*

Determination of heats of adsorption;

$\log\left(\frac{\theta}{1-\theta}\right) versus \frac{1}{T}$ is plotted for each concentration and $-\frac{Q_{ads}}{2.303R}$ as the slope is used to Calculate the heats of adsorption. Below is the equation used

$$\log\left(\frac{\theta}{1-\theta}\right) = \log A + \log K - \frac{Q_{ads}}{2.303R}\left(\frac{1}{T}\right) \quad (18)$$

Where θ *= Surface coverage of inhibitor* (Obi-Egbedi *et al*., 2012).

Gibbs energy of adsorption is calculated using the formula below

$$\Delta G = -RT \ln(55.5K)$$

Where,

$$K = \frac{\theta}{\left[(1-\theta)C\right]} \quad (19)$$

Θ= Degree of surface coverage, K= Adsorption equilibrium constant, C= Concentration (Kini *et al.*, 2011).

In order to study the interaction (mechanism of adsorption) between the metal (aluminium) and inhibitor molecules; various adsorption isotherms have been tested. The adsorption taken place follows the Langmuir adsorption isotherm by having a high correlation coefficient. It obeys the following equation.

$$\frac{C}{\theta} = \frac{1}{K} + C \quad (20)$$

Other isotherms tested and equations used

Frumkin isotherm

$$\left(\frac{\theta}{1-\theta}\right)\exp\left(-2a\theta\right) = KC \quad (21)$$

Temkin isotherm

$$\exp(-2a\theta) = KC \quad (22)$$

Freundlich isotherm

$$log\,\theta = log K + n log C \quad (23)$$

Where C= Concentration, Θ = Degree of surface coverage, $a_=$ molecular interaction parameter, $n_=$ Slope, K= Equilibrium constant of adsorption (Fouda *et al.,* 2012; Lebrini *et al.,* 2013; Arockiasamy *et al.,* 2014).

2.2 Materials and methods

2.2.1 Materials preparation

(i) Sample collection

Carica papaya leaves used in this investigation were collected from farms of villagers around our campus, Tengeru area, Arumeru District in Arusha, Tanzania. They were air dried for two weeks, then ground by an electrical grinder to a fine powder.

(ii) Preparation of an extract

In each of the batch experiments conducted at specific temperatures, three liters (3 L) of 1.0 M H_2SO_4 were firstly prepared and then used to prepare the extract and the corrosive media. Inhibitor (the extract) preparation was done by mixing two liters (2 L) of the acid with 200 g of the *C. papaya* leaves powder into two different one liter (1 L) pyrex conical flasks, in a ratio of 10 g of the leaves powder per 100 ml of the acid. This ratio was taken because on testing various ratios, it was found to be most efficient. The mixture obtained was boiled at

90˚C using a heating plate for three hours with a stir (Thermometer was used to maintain such temperature). Then it was left to cool at room temperature for 24 hours and thereafter filtered by firstly using a sieve followed by a centrifuge and finally with Whatman No. 1 filter papers. After filtering, the obtained solution was a corrosion inhibitor (itself with 100 v/v% concentration). From that inhibitor, other concentrations (20, 40, 60, and 80) v/v% were prepared by diluting it with the remained one liter (1 L) of 1.0 M H_2SO_4 at various ratios (Avwiri and Igho, 2003; Leelavathi and Rajalakshmi, 2013a; Prabhu, 2013; Loto *et al.*, 2014; Nwosu *et al.*, 2014).

(iii) Aluminium coupons preparation

The coupons with 2 cm × 2 cm × 0.12 cm in dimensions were filed by using emery papers (#400, 600, 800, 1000, and 1200), washed with ethanol, dried with acetone, and then stored in desiccators until used. Elemental composition of aluminium material used to prepare the coupons (Table 1) was determined using Wavelength-dispersive X-ray fluorescence Spectroscopy (WDXS).

Table 1: Elemental composition of aluminium material used (%)

Element	%	Element	%
Al	98.94	**Cu**	0.004
Mg	0.35	**Cr**	0.0029
Si	0.34	**P**	0.002
Fe	0.26	**Mn**	0.0017
Ti	0.0097	**Ag**	0.0004
Ni	0.0008	**Pb**	0.0004
V	0.0069	**Co**	0.0003
Zn	0.004		

2.2.2 Gravimetric analysis (Weight loss measurements)

In this method, a Denver analytical balance with an accuracy of 0.0001 g was used. Coupons' weights were measured before and after they have been immersed in the corrosive media. Distilled water, ethanol, acetone and desiccators were used to wash and dry the coupons several times before taking measurements.

In every batch experiment, each coupon was immersed for 24 hours in a 150 ml beaker. The total volume of the medium in each beaker was made up to 100 ml. The experiments were done at concentrations of a blank, (20, 40, 60, 80 and 100) v/v% and temperatures of 303 K, 313 K and 323 K. All beakers were put in water baths to control such temperatures. The experiments were repeated three times and the average weights lost were recorded and then well analysed.

2.2.3 Surface characterization

Surface morphology was examined using a Field Scanning Electron Microscope (FE-SEM, Hilachi, S-4700). BRUKER FTIR spectrometer in transmittance mode with a spectral range of 4000 – 500 cm^{-1} was used to ascertain functional groups of the extract associated with corrosion inhibition action.

2.3 Results

Refer to Appendix I and III; equations 13, 14 and 15 were used on determining the values in table 2 below:

2.3.1 Weight loss, inhibition efficiency and corrosion rate values

Table 2 and Fig.1 show that inhibition efficiency increases with increase in concentration and decreases with the rise in temperature. The maximum inhibition efficiency at 303 K, 313 K and 323 K is 71.67 %, 67 and 58.64 % respectively. The concentration at which the maximum adsorption has taken place (optimal concentration) of inhibitor at 303 K, 313 K and 323 K is 60 %, 80 % and 60 % v/v respectively.

Table 2: Shows the average weight loss and calculated corrosion rate for each experiment

Conc. (v/v %)	*Weight loss (g) and Inhibition efficiency*						*CR ($gcm^{-2}h$) (10^{-5})*		
	303 K	**I.E %**	**313 K**	**I.E%**	**323 K**	**I.E%**	**303 K**	**313 K**	**323K**
Blank	0.012		0.0359		0.0856		5.580	16.695	39.807
20	0.0049	59.17	0.015	58.32	0.0428	50.00	2.279	6.975	19.903
40	0.0038	68.33	0.013	63.88	0.0378	55.84	1.767	6.045	17.578
60	0.0034	71.67	0.0122	65.98	0.0354	58.64	1.581	5.673	16.462
80	0.0034	71.67	0.0118	67	0.036	57.94	1.581	5.487	16.741
100	0.0036	70.00	0.0126	65.9	0.0384	55.14	1.674	5.859	17.857

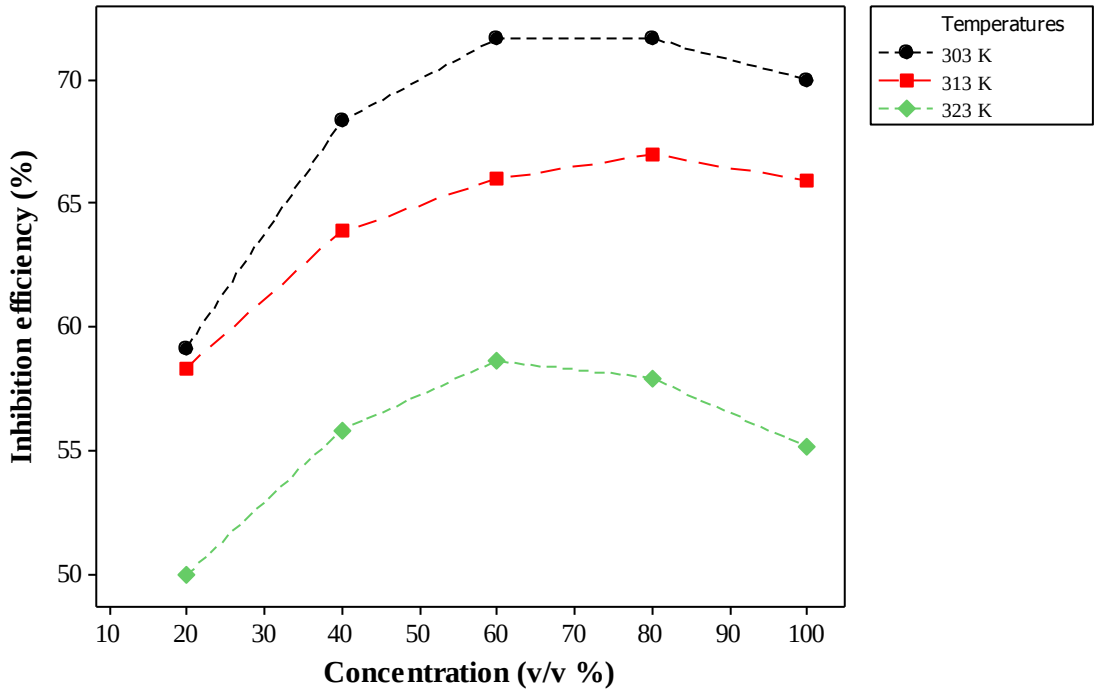

Figure 1: The relationship between inhibition efficiency and concentration at various temperatures

2.3.2 Kinetic and thermodynamic parameters

Kinetic and thermodynamic parameters include activation energy—E_a (J/mol), enthalpy of activation—$+\Delta H\ kJ/mol$, the entropy of adsorption—ΔS^0 (J/mol), heat energy of

adsorption— ΔQ_{ads} (kJ/mol and Gibbs energy of adsorption— ΔG^{0} (J/mol) were determined and recorded in Table 3. Determination of activation energy was done by plotting the graphs of ln (Corrosion rate) vs1/Temperature using equation (16). Their slopes $-\frac{E_a}{R}$ obtained were then used in calculations (Fig. 2 indicates the summary graph at various concentrations of the inhibitor). Enthalpy of activation and entropy of adsorption were determined by plotting graphs of ln (Corrosion rate/Temperature) vs 1/Temperature using equation (17), then $-\frac{\Delta H^{0}}{R}$ as slopes to calculate the enthalpy of activation and $\ln\left(\frac{R}{Nh}\right)+\frac{\Delta S^{0}}{R}$ as intercepts to calculate the entropy of adsorption (Fig. 3 is the summary graph at various concentrations). Heats of adsorption were determined by plotting graphs of Log [Surface coverage/(1-Surface Coverage)] using equation (18), and $-\frac{Q_{ads}}{2.303R}$, as slopes were used in calculations (Fig 4 is the summary graph at all concentrations of inhibitor (0%, 20%, 40%, 60%, 80% and 100%). Gibbs energy of adsorption was determined using Equation (18).

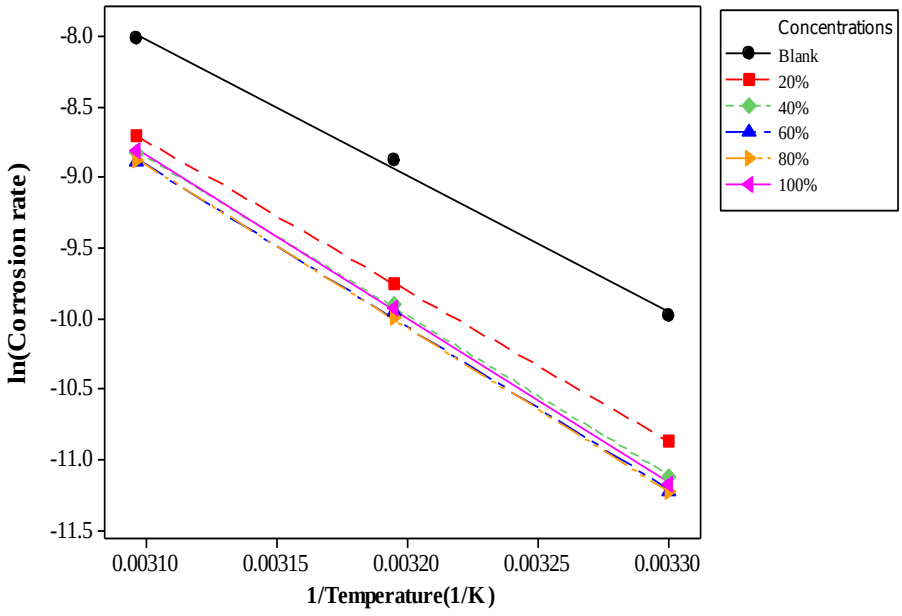

Figure 2: A plot of ln (Corrosion rate) vs 1/Temperature

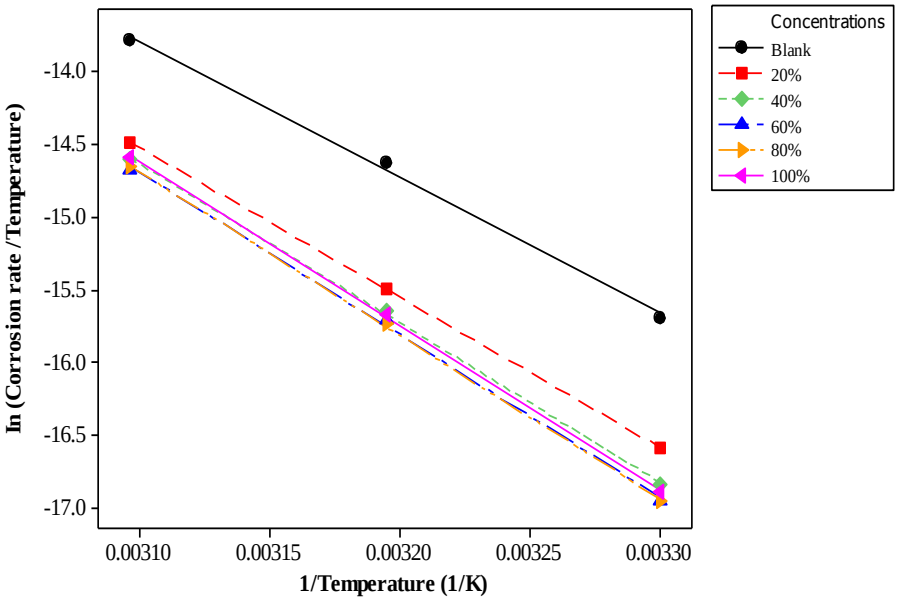

Figure 3: A plot of ln (Corrosion rate/Temperature) vs 1/Temperature

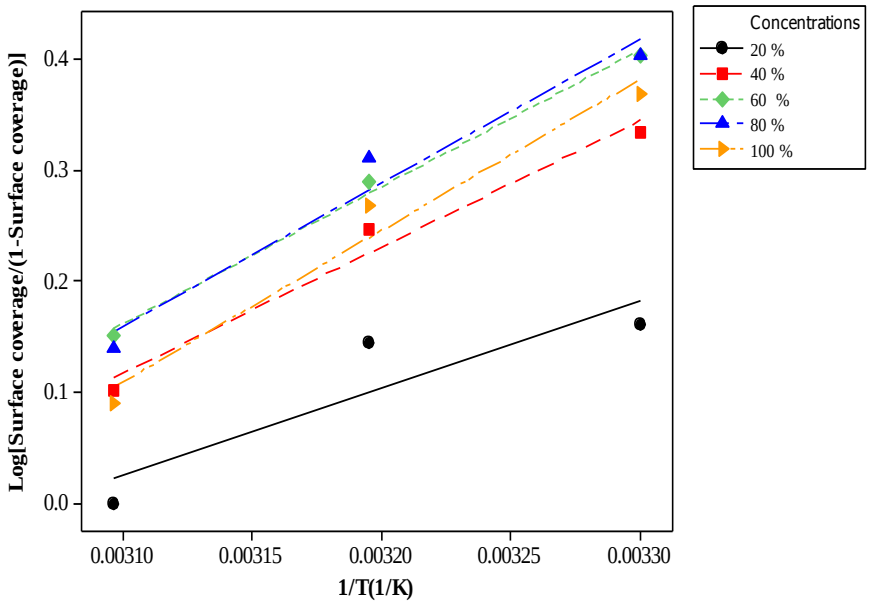

Figure 4: A plot of Log [Surface coverage/(1-Surface Coverage)]

Table 3: Shows kinetic and thermodynamic parameters

Conc. v/v %	E_a ***kJ/mol***	$+\Delta H$ ***kJ/mol***	ΔS^0 ***J/mol***	ΔQ_{ads} ***(kJ/mol)***	ΔG ***(kJ/mol)***		
					303 K	313K	323K
Blank	80.01	77.40	-70.75				
20	88.18	85.58	-51.46	14.96	-3.51	-3.53	-2.74
40	93.50	86.42	-35.92	21.67	-2.76	-2.34	-1.51
60	95.38	92.78	-30.59	23.51	-2.14	-1.52	-0.73
80	96.03	93.42	-28.52	24.64	-1.42	-0.89	0.12
100	96.33	93.73	-27.02	26.00	-0.65	-0.18	1.03

2.3.3 Adsorption isotherms

Since the inhibitor works through adsorption onto the metal surface, various adsorption isotherms were tested includes Langmuir, Frumkin, Temkin and Freundlich adsorption isotherms using equations; 20, 21, 22 and 23 respectively. Table 4 shows correlation coefficient values for each isotherm at various temperatures as have been tested.

The adsorption of the inhibitor onto the metal surface seems to obey Langmuir adsorption isotherm by having a high correlation coefficient of approximately equal to 1. This isotherm goes with the assumption that, there is no lateral interaction between the adsorbed species and the adsorbent. Fig. 5 shows the Langmuir adsorption isotherm plot.

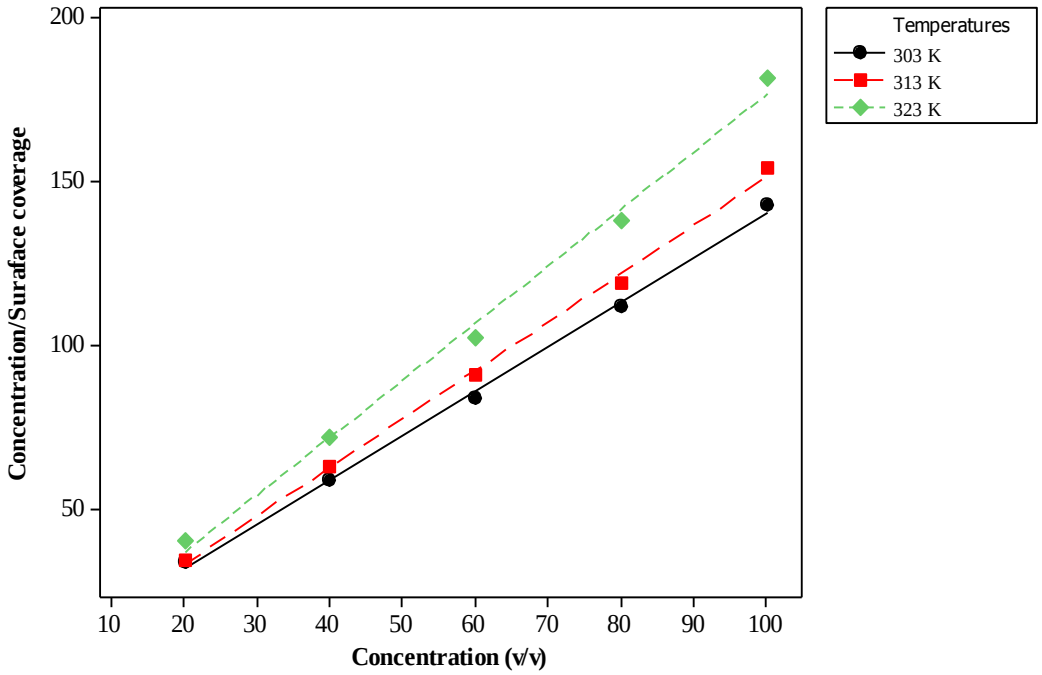

Figure 5: Langmuir adsorption isotherm plot at various temperatures

Table 4: A summary of correlation coefficients for the isotherms tested

Isotherm	***Correlation coefficient value (R^2) at various temperatures***		
	303K	*313K*	*323K*
Frumkin	0.561	0.794	0.383
Freundlich	0.786	0.869	0.565
Temkin	0.787	0.873	0.553
Langmuir	0.997	0.998	0.995

2.3.4 FT-IR spectroscopy analysis

FT-IR test was performed to the *C. papaya* leaves powder, inhibitor prepared by using 1.0 M H_2SO_4 and the corrosion product (adsorbed film). In case of the leaves powder a little amount of the sample was tested and in corrosion inhibitor, few drops were tested. A test concerning a corrosion product was done by firstly preparing the aluminium coupon. The coupon was prepared by being abraded with emery papers, then washed with ethanol and dried with acetone. The prepared coupon was immersed in 60 v/v% inhibitor (optimal concentration) in

100 ml of the medium (150 ml beaker was used), for 24 hrs at 30˚C. Then after, a coupon was scrapped to get a corrosion product which was FT-IR tested. The results obtained here were the FT-IR spectra of the *C. Papaya* leaves, inhibitor and the corrosion product shown in Figs. 6-8 respectively.

Table 5 shows functional groups identified from *C. papaya* leaves powder, inhibitor prepared by using H_2SO_4 and the corrosion product (adsorbed film) using FT-IR spectroscopy. Absorption frequencies in the table are the values recorded from the FT-IR spectra (Figs. 6-8).

Table 5: FT-IR Spectroscopy results (H_2SO_4 medium)

Leaves powder		**Inhibitor prepared using H_2SO_4**		**Corrosion product**	
Frequency (cm^{-1})	Assignment	Frequency (cm^{-1})	Assignment	Frequency (cm^{-1})	Assignment
3281.43	-OH or N-H Stretch	3334.5	O-H Stretch	3329.84	O-H Stretch
2917.52	-C-H Stretch	1634.65	C=O Stretch	1635.23	C=O Stretch
2849.24		1189.41	C-O or C-H Stretch	1183.08	C-O or C-N Stretch
1625.62	C=O stretch	1049.60		1048.00	
1405.52	C-H bending				
1316.22					
1244.02	C-O or C-N stretch				
1031.06					

Figs. 6, 7 and 8 are FT-IR Spectra for *C. Papaya* leaves, inhibitors and their adsorbed film;

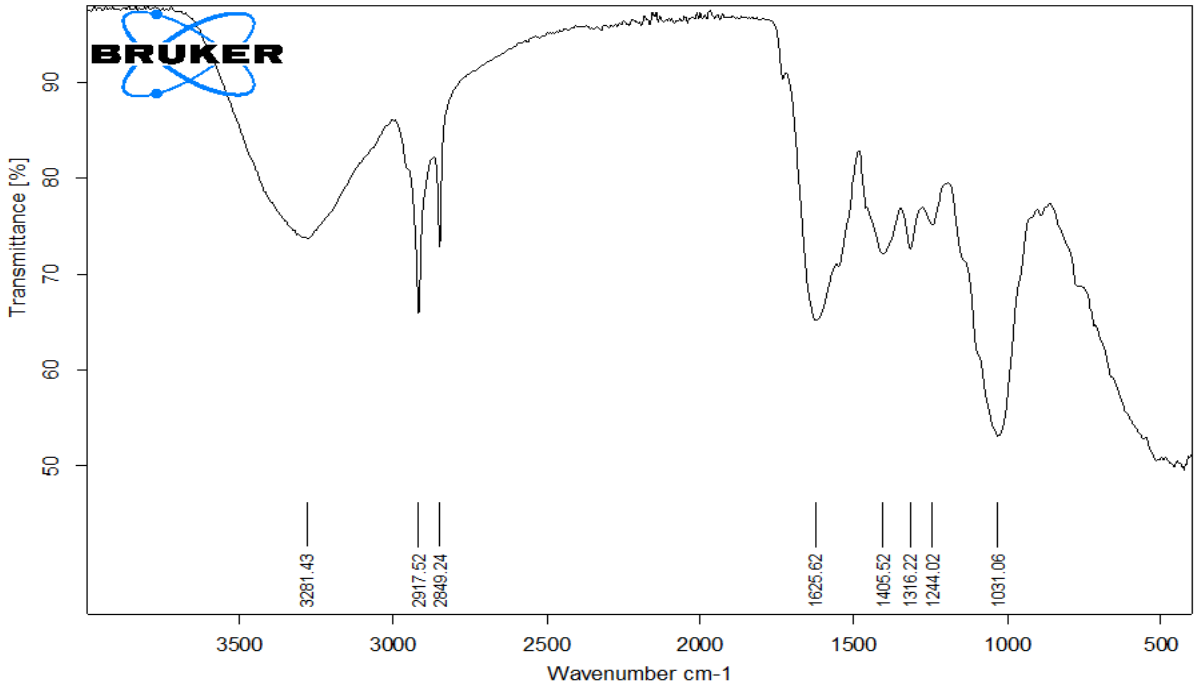

Figure 6: FT-IR spectrum for the *C. papaya* leaves powder

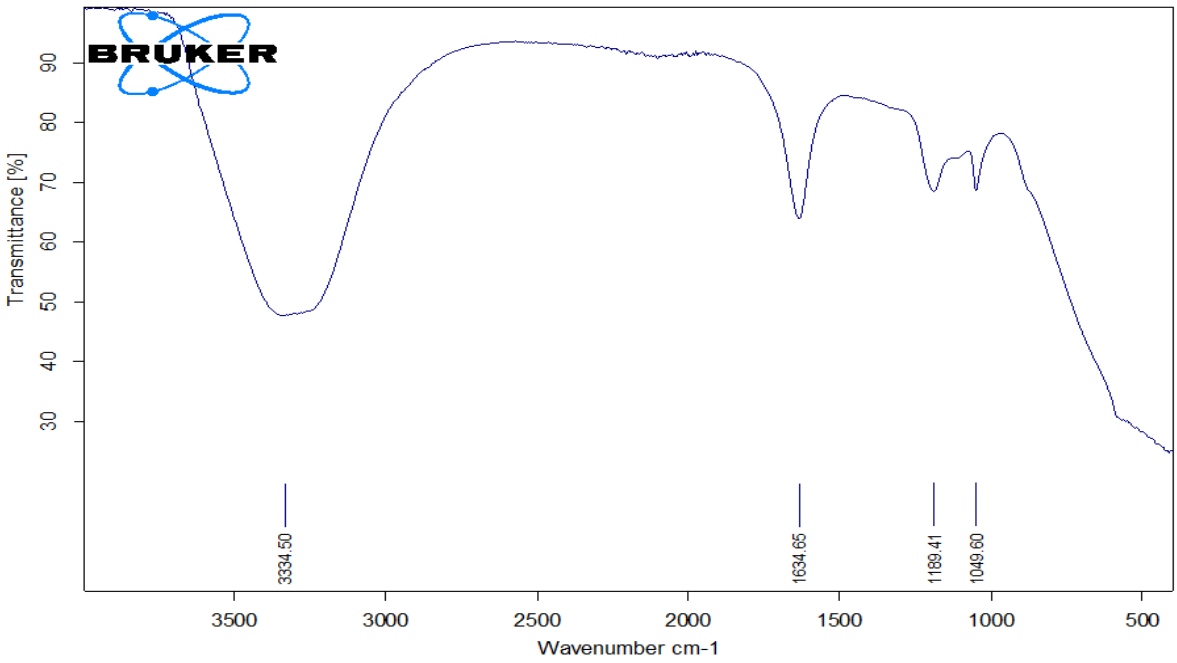

Figure 7: FT-IR spectrum for the inhibitor prepared using H_2SO_4

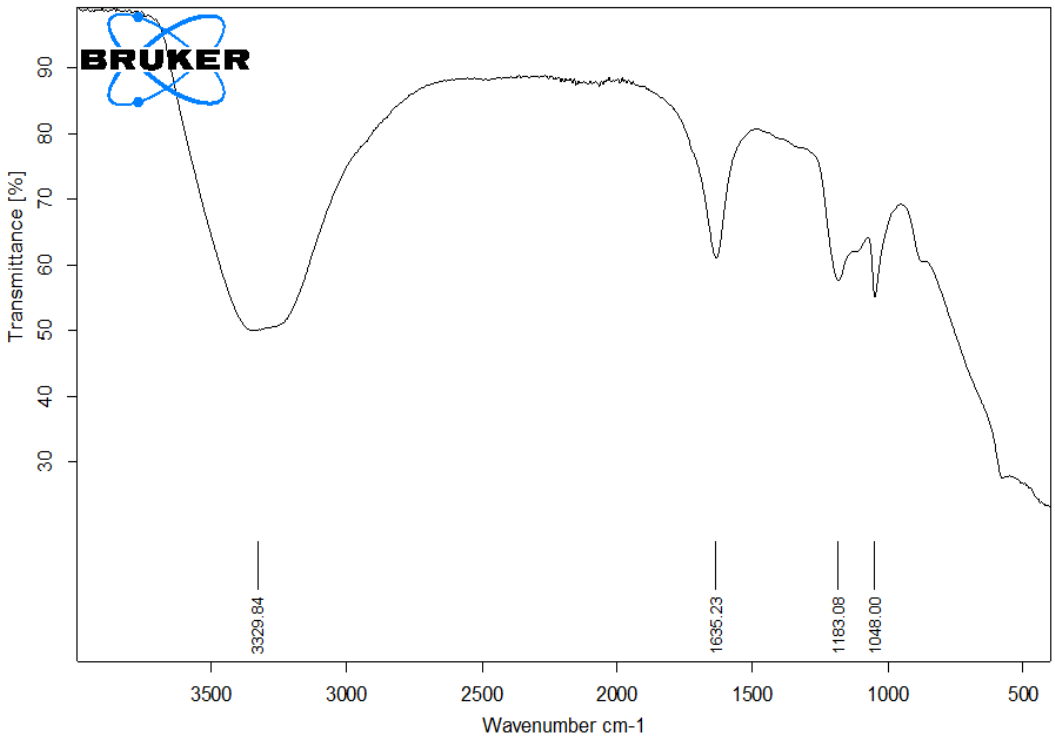

Figure 8: FT-IR Spectrum indicating the adsorbed film formed after using H_2SO_4

The functional groups assigned from *C. papaya* leaves, prepared inhibitor and adsorbed film, are those functional groups found to participate in the adsorption and inhibition of various inhibitors which have been reported. The shift of these frequencies from an inhibitor to the adsorbed ones can be attributed to the interaction of inhibitor functional groups with the metal surface for the adsorption to take place. For example, O-H vibration was shifted from 3334.5 cm^{-1} to 3329.84 cm^{-1} and that of C=O from 1634.65 cm^{-1} to 1635.23 cm^{-1} (Eddy, 2009; Sangeetha *et al.*, 2012; A Negm *et al.*, 2013; Leelavathi and Rajalakshmi, 2013b; Odewunmi *et al.*, 2015). The difference in SEM images of the aluminium surface by the one with an inhibitor to be smoother than the surface of without it is also a proof of the inhibitor adsorption as well as its activeness (Kini *et al.*, 2011; Arellanes-Lozada *et al.*, 2014).

2.3.5 Surface profile analysis using SEM

Uncorroded, uninhibited and inhibited coupons were examined by using Scanning Electron Microscope (SEM). Uninhibited and inhibited coupons were dipped in the medium (100 ml of 1.0 M H_2SO_4) for 24 hours at 30˚C before analysis. For inhibited coupon, the inhibitor was added at the optimal concentration of 60 v/v%.

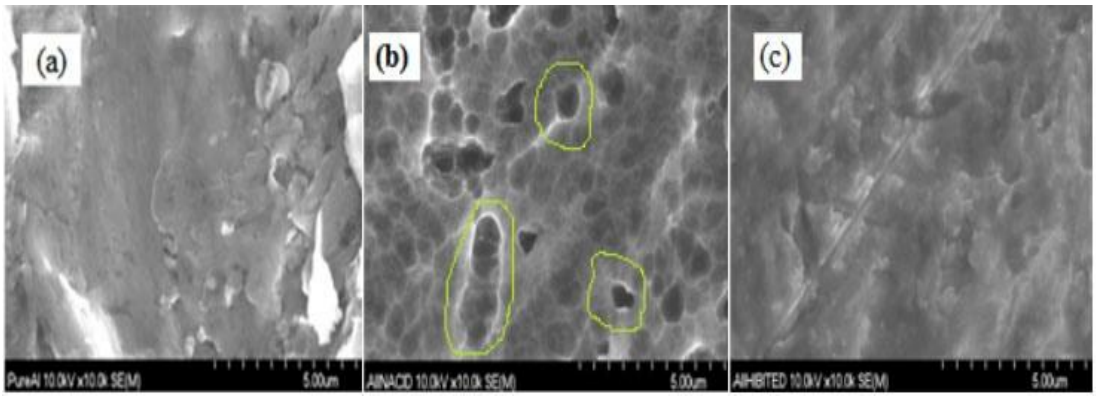

Figure 9: SEM images of aluminium coupons at various conditions

From Fig. 9 above coupons with different treatment displayed different images from SEM; (a) Uncorroded surface of aluminium coupon without pits, but some scratches which occurred during filing (b) Uninhibited coupon with deep pits (some of them are overlaid by the lines in order to become easily seen) shows corrosion has taken place (c) Inhibited coupon which shows the protected surface which is not much affected by the acid. From the surface profile of aluminium coupons done, the difference indicated above proves the formation of the adsorbed layer (film) which acted as a barrier to the acid corrosiveness.

2.4 Discussion and conclusion

The increase in the activation energy of the metal dissolution was due to the increase in the inhibitor concentration and its adsorption. This is because the inhibitor adsorption on the metal surface hindered the metal dissolution (Obot *et al.*, 2011; Hamdy and El-Gendy, 2013). The positive values of enthalpy of activation show the endothermic nature of the metal dissolution which is associated with the rise in corrosion rate of the metal at high temperatures (Quraishi *et al.*, 2010). Increasing in entropy (from most negative to less negative values), shows the increase in disorder at the metal and solution interface which is due to the desorption of water molecules from the surface of the metal by molecules of the inhibitor (Quraishi *et al.*, 2010). The increase in the heats of adsorption with the increase in concentration of the inhibitor shows the exothermic nature of its adsorption. Gibbs energy increased (from most negative to less negative) as the temperature rises also implies the exothermic nature of the adsorption process (Obot *et al.*, 2011). This means that at high temperature there was desorption of the inhibitor on the metal surface (Obi-Egbedi *et al.*, 2012). Adsorption isotherms together with the kinetic and thermodynamic parameters helped to determine whether the adsorption process was achieved through the physical or chemical

mechanism. In the current study, all parameters agreed to physical adsorption of the inhibitor on the metal surface.

The functional groups assigned from *C. papaya* leaves, prepared inhibitor and adsorbed film; are those functional groups found in most of inhibitors to participate in adsorption and corrosion inhibition. The shift of these frequencies from inhibitor to the adsorbed ones can be attributed to the interaction of inhibitor functional groups with the metal surface for adsorption to take place (Eddy, 2009; Sangeetha *et al.*, 2012; A Negm *et al.*, 2013; Leelavathi and Rajalakshmi, 2013b; Odewunmi *et al.*, 2015).

From the surface profile of aluminium coupon done, the difference indicated above proves formation of the adsorbed layer (film) which acted as a barrier to the acid corrosiveness (Kini *et al.*, 2011; Arellanes-Lozada *et al.*, 2014).

Various investigations concerning *C. Papaya* leaves as a green corrosion inhibitor either with synergism or not, indicated the moderate to high inhibition efficiency depending on the type of the medium and the metal under investigation. The reported findings show inhibition efficiency values as following, *C.papaya* extracts on the corrosion of mild steel (Okafor and Ebenso, 2007), 93.88 % at a concentration of 2g/L, inhibition effect of extracts of *C. papaya* and camellia sinensis leaves, 68.97% at 100 v/v % (Loto *et al.*, 2011), synergistic effects of *C. papaya* leaves extract with Zn^{2+} in corrosion inhibition of mild steel in an aqueous medium, 91 % by 2ml *C. papaya* leaves (CPL) extract with Zn^{2+} (50 ppm) in 100 mL (Kavitha *et al.*, 2014). Performance of mild steel in nitric acid/*C. Papaya* leaf extracts corrosion (Oki *et al.*, 2015) with 92.8 % efficiency at 60 % v/v %. The current study reports a maximum inhibition efficiency of 71.67 % at its optimal concentration of 60 v/v %. In comparison between the efficiency of the *C. papaya* extracts in the current study and the previous ones shown above, it still shows the extract can bring out inhibitive properties of corrosion under various media to the different kinds of metals.

2.5 Acknowledgements

This work was supported by the Government of Tanzania through Nelson Mandela African Institution of Science and Technology.

CHAPTER THREE

GREEN APPROACH TO CORROSION INHIBITION OF ALUMINIUM BY *Carica Papaya* LEAVES EXTRACT IN PHOSPHORIC ACID

Abstract

The inhibitive ability of C. *Papaya* leaves in corrosion of aluminium in 1.0 M Phosphoric acid was investigated using a weight loss method at various concentrations and temperatures 303K, 313K and 323K. Inhibition efficiency was found to decrease with the increase in temperature and increases with the increase in concentration and fits well to the Langmuir adsorption isotherm. Thermodynamic and kinetic parameters were also determined and found to agree with physical adsorption as a mechanism of corrosion inhibition.

Keywords: *C. papaya*, inhibition, aluminium, phosphoric acid, adsorption, thermodynamic and kinetic parameters

3.1 Introduction

Investigation of various materials to be used as corrosion inhibitors of metals has been increasing nowadays. This is due to various applications which need the introduction of those inhibitors to ensure the metals safety**.** Those applications include: acid descaling, acid pickling, acid cleaning, oil well acidization and electro polishing (Ladha *et al.;* Yurt *et al.*, 2006). Synthetic and natural materials have been investigated for several years, but synthetic ones have been associated with toxicity which interferes with human biochemical reactions and some of the organs such as livers and kidney. Good examples of this are the chromium compounds (chromates) which have been reported to be carcinogenic (Rani and Basu, 2011; Kesavan *et al.*, 2012). This motivated most of the corrosion engineers to shift most of the studies into natural materials since they are environmentally and ecologically safe (Kesavan *et al.*, 2012; Singh *et al.*, 2012). Plant extracts are among those natural materials which are rich in phytochemicals being adsorbed onto the metal surface under a corrosive medium to cause corrosion inhibition. They are also cheap, locally available and renewable (Singh *et al.*, 2012).

The essence of investigating inhibition of aluminium dissolution in phosphoric acid is that the acid has been used in aluminium cleaning and electropolishing where inhibitors are needed (Ali and Foaud, 2012). Several studies concerning inhibition of aluminium corrosion in phosphoric acid using natural materials have been done. Among of them include the synergistic effect of iodide and purine (Amin *et al.*, 2009b), synergistic effect of chalcones derivatives and halide ions (Fouda *et al.*, 2013), *G. Indica* (Prabhu and Rao, 2013) and *D. brandisii* (Li and Deng, 2012). This Chapter discusses the corrosion inhibition of aluminium under phosphoric acid by using *C. Papaya* as a natural (green) inhibitor.

3.2 Materials and methods

The same sample collected, aluminium coupons preparation, media preparation, and experimental setup were used as in Chapter 2. Preparation of inhibitor was done by Refluxing (boiling) *C. papaya* leaves powder with phosphoric acid (H_3PO_4) at 90^0C. The mixture was then allowed to cool for 24 hours before filtering to get a corrosion inhibitor. The medium was prepared and then used in the weight loss method. The experiments were repeated three times at concentrations of Blank, (20, 40, 60, 80 and 100) v/v % and temperatures of 303 K, 313 K and 323 K. All processes and conditions were the same as what was done by using sulphuric acid (H_2SO_4), reported in Chapter 2.

From the gravimetric analysis (weight loss method) data, inhibition efficiency, the degree of surface coverage, corrosion rate, enthalpy and entropy of activation, Gibbs energy, heat of adsorption and adsorption isotherm were determined as in Chapter 2.

3.3 Results

Refer to Appendix II and IV; equations 13, 14 and 15 were used in determining the values in Table 6 below.

3.3.1 Weight loss results, inhibition efficiency and corrosion rate values

Table 6 and Fig.10 show that inhibition efficiency increases with increase in concentration and decreases with the rise in temperature. The maximum inhibition efficiency at 303 K, 313 K and 323 K is 56.02%, 49.82% and 41.99% respectively. The concentration at which maximum adsorption has taken place (optimal concentration) of inhibitor at 303 K, 313 K and 323 K is 80%, 80% and 60% v/v respectively.

Table 6: Shows weight loss and calculated corrosion rate

Conc. (v/v %)	***Weight loss (g)***						***CR($gcm^{-2}h^{-1}$) (10^{-5})***		
	303 K	**I.E %**	**313K**	**I.E%**	**323K**	**I.E%**	**303 K**	**313K**	**323K**
Blank	0.0698		0.1704		0.3491		3.2459	7.9241	16.2342
20	0.0391	43.98	0.0988	42.02	0.2191	37.24	1.8183	4.5945	10.1888
40	0.0334	52.15	0.0925	45.72	0.2107	39.64	1.5532	4.3015	9.7982
60	0.0316	54.73	0.087	48.94	0.2025	41.99	1.4695	4.0458	9.4169
80	0.0307	56.02	0.0855	49.82	0.2063	40.91	1.4276	3.9760	9.5936
100	0.0308	55.87	0.0866	49.18	0.2070	40.70	1.4323	4.0272	9.6261

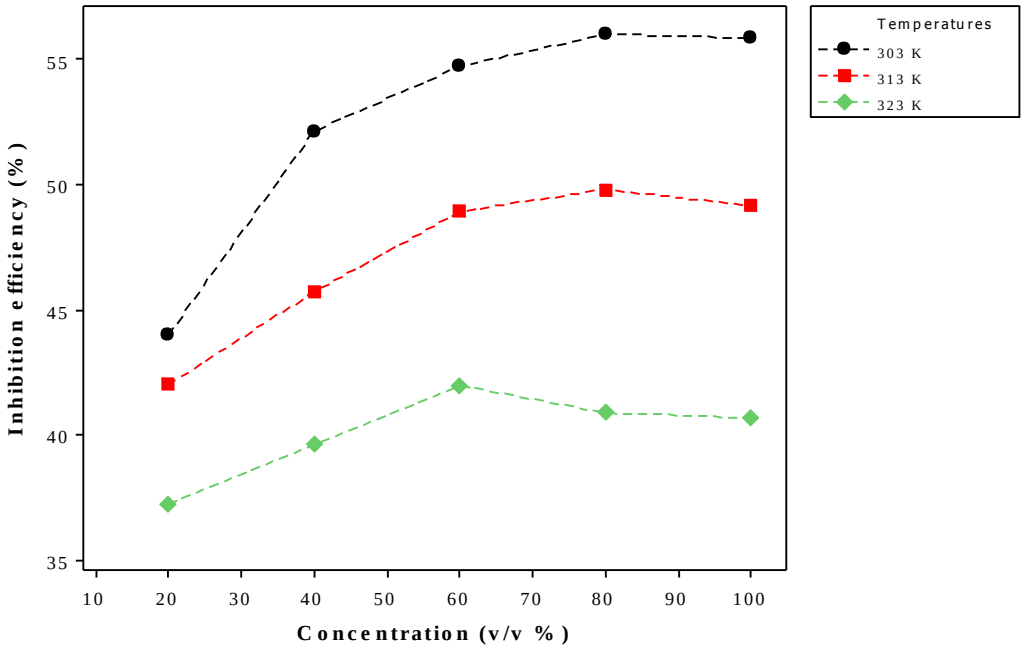

Figure 10: A graph shows the variation of inhibition efficiency with a concentration of inhibitor

3.3.2 Thermodynamic and kinetic parameters

Table 7 Shows, kinetic and thermodynamic parameters which are activation energy— E_a *(kJ/mol*), enthalpy of activation— $+\Delta H$ *(kJ/mol),* the entropy of adsorption (activation)— ΔS^0 *(J/mol),* heat energy of adsorption —ΔQ_{ads} *(kJ/mol)* and Gibbs energy of adsorption — ΔG *(kJ/mol).* Equations 16, 17 and 18 were used to plot graphs, then slopes and intercepts used in calculations. Graph number 11, 12 and 13 are the summary graphs at all concentrations 0, 20, 40, 60, 80, 100 on which the inhibitor was tested.

Table 7: Thermodynamic and kinetic parameters

Conc. V/v %	E_a ***kJ/mol***	$+\Delta H$ ***kJ/mol***	ΔS^0 ***J/mol***	ΔQ_{ads} ***(kJ/mol)***	ΔG ***(kJ/mol)***		
					303 K	313K	323K
Blank	65.55	62.95	-103.92				
20	70.15	67.55	-93.62	11.34	-1.96	-1.82	-1.34
40	74.99	72.40	-78.82	20.60	-1.04	-0.41	0.25
60	75.62	73.02	-77.24	20.85	-0.28	0.31	1.08
80	77.54	74.94	-71.25	24.76	0.31	0.97	1.97
100	77.55	74.96	-71.08	24.87	0.89	1.62	2.59

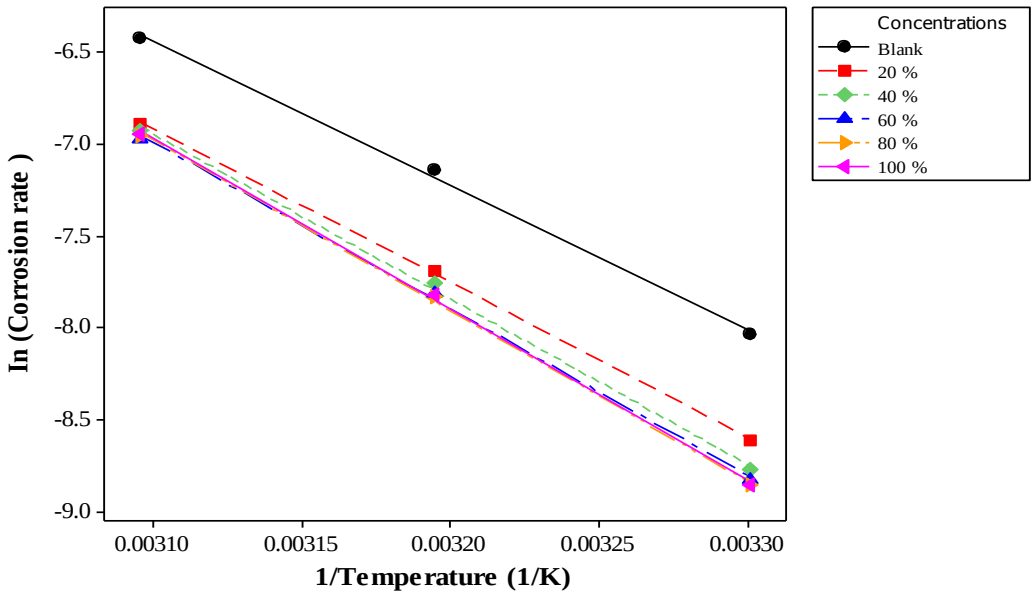

Figure 11: The graph in summary used in determination of activation energies

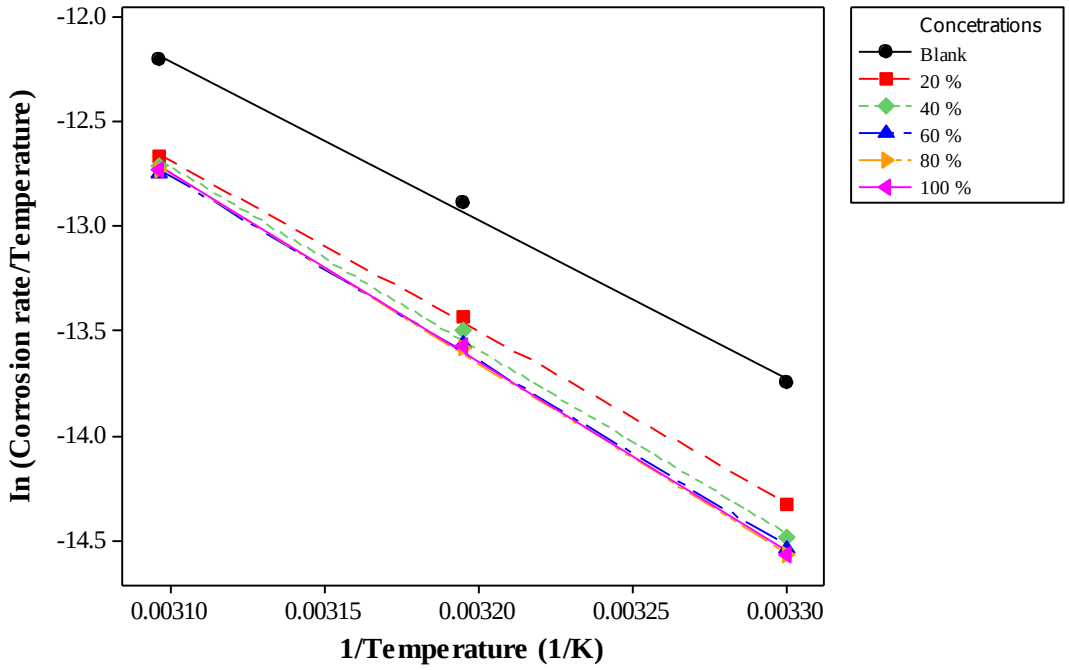

Figure 12: The graph in summary used in determination of the enthalpy and entropy of activation

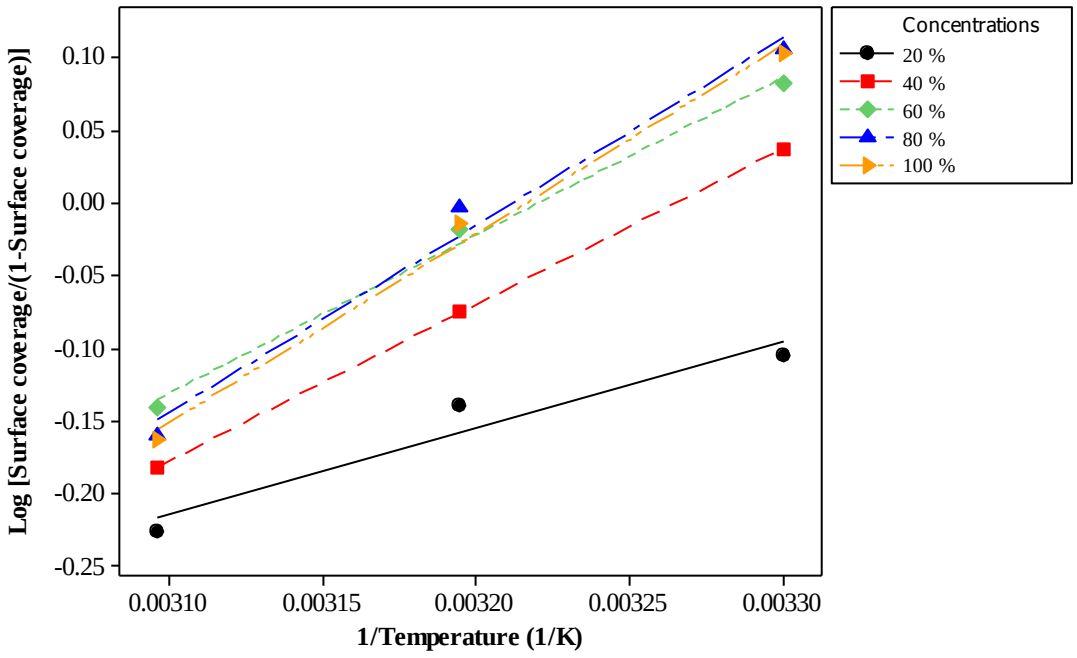

Figure 13: The graph in summary used in determination of heats of adsorption

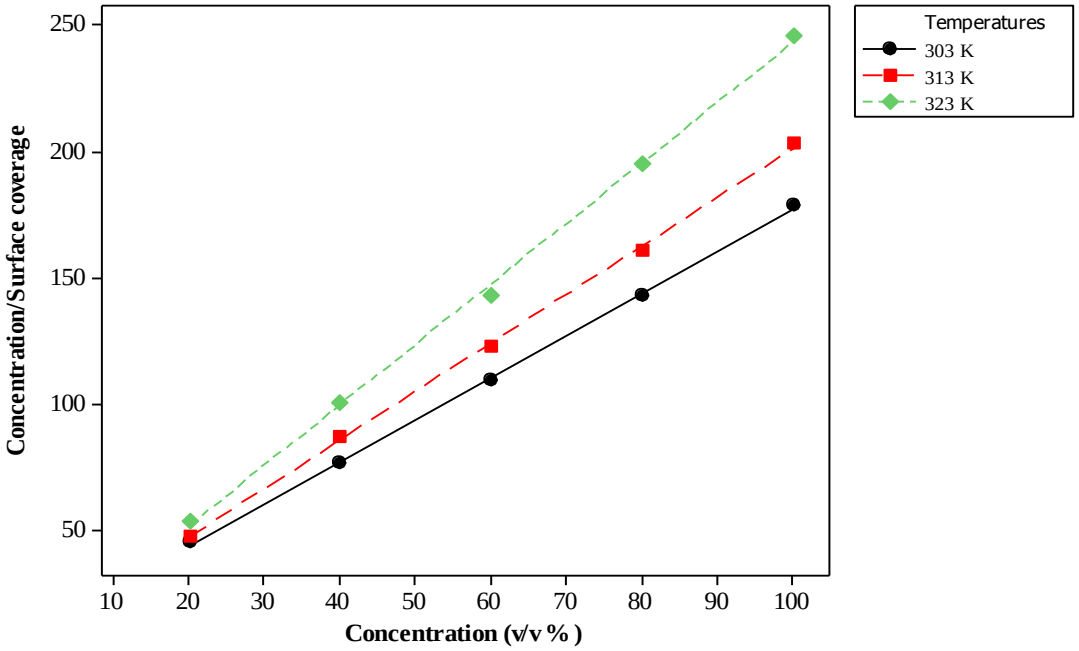

Figure 14: A graph for the Langmuir adsorption isotherm at various temperatures

Table 8: A summary of correlation coefficients for the isotherm tested

Isotherm	***Correlation coefficient value (R^2) at various temperatures***		
	303K	*313K*	*323K*
Frumkin	0.835	0.888	0.647
Freundlich	0.907	0.928	0.713
Temkin	0.919	0.928	0.713
Langmuir	0.999	0.999	0.999

Table 8 shows correlation coefficients of the isotherms tested. The adsorption process follows Langmuir adsorption because of the highest correlation coefficient of approximately equal to 1. Equations; 20, 21, 22 and 23 were used in plotting graphs and determination of the best isotherm. Fig. 14 is a summary graph of the Langmuir adsorption isotherm at various temperatures.

3.3.3 FT-IR spectroscopy results

The functional groups have been assigned from the *Carica papaya* leaves, corrosion inhibitor and a corrosion product as done in Chapter 2. In case of a corrosion product; aluminium coupon was well prepared by being abraded accordingly, and then immersed in 60 v/v %

inhibitor (1.0 M H_3PO_4 medium was used) for 24 hours. Then after, a corrosion product was well scrapped for the FT-IR test. The results obtained here were the FT-IR spectra shown in Figs. 15-17. From these spectra, the respective absorption frequencies were recorded in Table 9. The shift of these frequencies between inhibitor prepared and the corrosion product reveal the interaction of inhibitor functional groups and the aluminium surface.

Table 9: FT-IR spectroscopy results (H_3PO_4 medium)

Leaves powder		**Inhibitor prepared using H_3PO_4**		**Corrosion product**	
Frequency (cm^{-1})	Assignment	Frequency (cm^{-1})	Assignment	Frequency (cm^{-1})	Assignment
3281.43	-OH or N-H Stretch	3333.77	O-H Stretch	3258.42	O-H Stretch
2917.52	-C-H Stretch	1635.58	C=O Stretch	1634.90	C=O Stretch
2849.24		1162.14	C-O or C-N Stretch	1074.49	C-O or C-N Stretch
1625.62	C=O stretch	1073.93			
1405.52	C-H bend	999.47	C-H bend	983.78	C-H bend
1316.22					
1244.02	C-O or C-N stretch				
1031.06					

Table 9 above shows absorption frequencies for *C. papaya* leaves, corrosion inhibitor and the corrosion product as observed from FT-IR Spectra.

Figs. 15, 16 and 17 are the FT-IR Spectra for *C. papaya* leaves, inhibitors and their adsorbed films

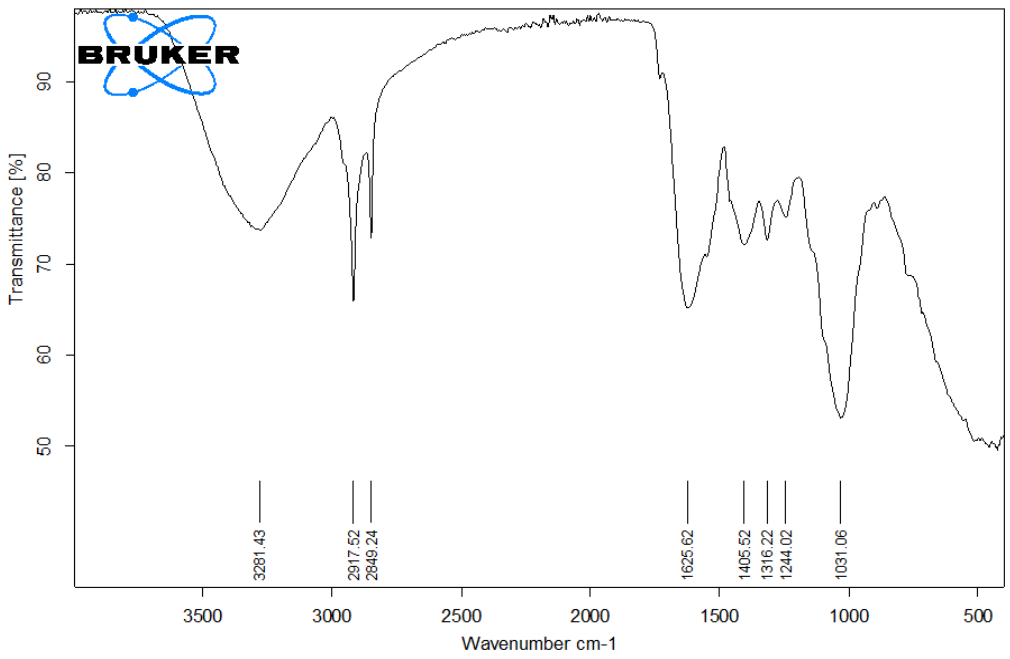

Figure 15: FT-IR Spectrum for the *C. Papaya* leaves powder

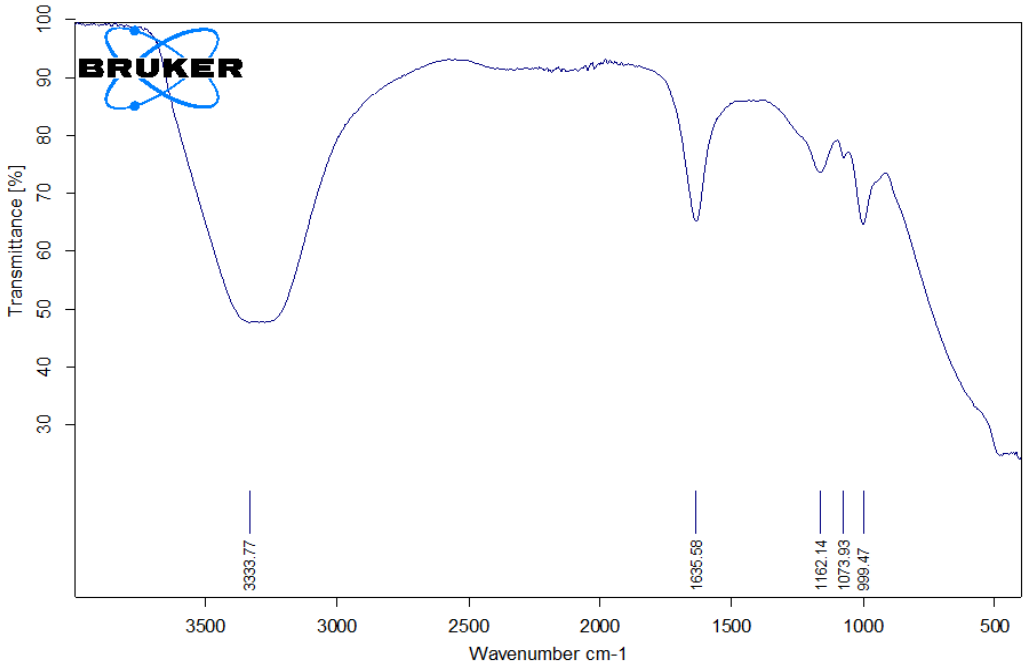

Figure 16: FT-IR spectrum for inhibitor prepared using H_3PO_4

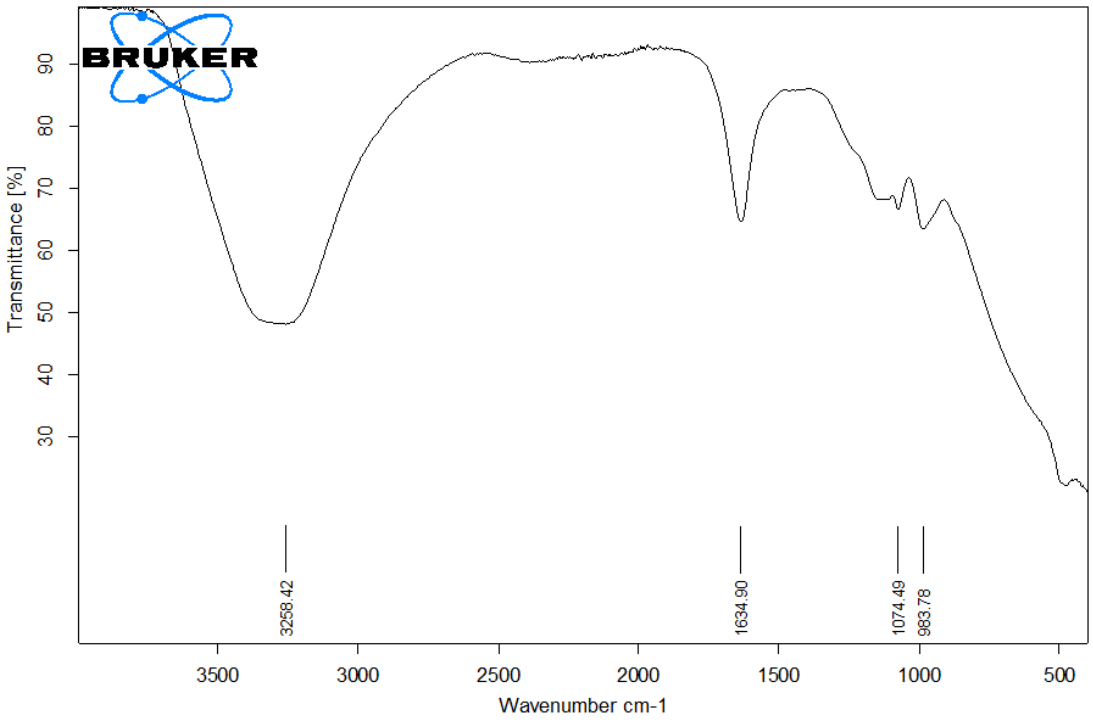

Figure 17: FT-IR spectrum for the adsorbed film formed after using H_3PO_4

3.4 Discussion and conclusion

Table 10 follows summarizes a discussion concerning kinetic and thermodynamic parameters determined in Table 7. In comparison with the parameters information discussed in Chapter 2, the values are in the similar trend, but different in numbers.

Table 10: Kinetic and thermodynamic parameters in summary

Thermodynamic and kinetic parameters	Value/ Change	Implication
Entropy	Increasing of entropy (from most negative to less negative values), shows the increase in disorder at the metal and solution interface.	This can be attributed to desorption of water molecules from the metal surface replaced with an inhibitor.
Gibbs energy	Increasing (from most negative to positive) as the temperature rises.	The exothermic nature of the inhibitor adsorption process which decreases at high temperature
Heats of Adsorption	The increase in heats of adsorption with the increase in concentration of inhibitor.	Exothermic nature of its adsorption.
Enthalpy of activation	The positive values of enthalpy of activation.	Reveals the endothermic nature of the metal dissolution.
Activation energy	The increase in activation energy with the increase in inhibitor concentration.	Means that, dissolution of the metal is not favoured at high concentration of the inhibitor.

All parameters analysed in table 10 above agreed to physical adsorption of inhibitor onto the metal surface. The inhibitor extract is adsorbed on the metal surface by displacing water molecules because it is organic material. Moles of water displaced (X) is proportional to the amount of inhibitor adsorbed. Equation 24, shows how this adsorption occurs (Amin *et al.*, 2009b; Fouda *et al.*, 2012; Prabhu and Rao, 2013).

$$\text{Org (sol)} + x\text{H}_2\text{O (ads)} \leftrightarrow \text{Org (ads)} + x\text{H}_2\text{O (sol)} \quad (24)$$

The functional groups of *Carica papaya* leaves powder, inhibitor and corrosion product assigned from FT-IR spectroscopy have excess electrons which make them act as an electron donor and the empty p-orbital of aluminium surface acts like electrons acceptor (Abd-El-Nabey *et al.*, 2012). The physical adsorption observed here happens through weak forces of attraction (Van der Waals forces) compared to chemical adsorption which occurs through chemical bonds.

Inhibition efficiency of 56.02 % at 80 v/v %, observed in this study (under H_3PO_4), is low compared to some of high efficient natural (organic) extract materials such as synergistic effect of iodide and purine with an efficiency of 92.05 % at 1× 10-2 M Purine (Amin *et al.*, 2009b) and chalcones derivatives and halides ions with an efficiency of 80.20 % at 1.0 $\times 10^{-2}$ M, KI and 11 $\times 10^{-6}$ M Chalcones (Fouda *et al.*, 2013), seed extract *D. brandisii* with an efficiency of 94.0 % at 1.0 g/L and *G. Indica* with 85.59 % efficiency at 500 ppm (Prabhu and Rao, 2013).

3.5 Acknowledgements

This work was supported by the Government of Tanzania through Nelson Mandela African Institution of Science and Technology.

CHAPTER FOUR

GENERAL DISCUSSION, CONCLUSION AND RECOMMENDATIONS

4.1 General discussion

The inhibitory effects of *Carica papaya* leaves extract in this investigation have closely related results in both sulfuric acid (H_2SO_4) and phosphoric acid (H_3PO_4) media. This is mainly due to the same method of preparing the extracts and the corrosive media used in the study are all acidic. From the FT-IR analysis, the observed functional groups of the prepared extracts show no much difference. It is only C-H which has been observed in H_2SO_4 and C-N in H_3PO_4 inhibitors. When comparing the amount of the functional groups in *Carica papaya* leaves and the extracts, leaves found to have a much more, this is due to the loss of some leaves constituents due to the temperature during boiling (refluxing).

Although isolation of *Carica papaya* phytochemicals and test of the active ones is not reported, compounds such as kaemphferal, myrecetin, quarcetin, and tannins, which are found in this plant extracts can be associated with the cause of inhibitive properties (Canini *et al.*, 2007; Radojčić *et al.*, 2008; Rahim and Kassim, 2008; James and Akaranta, 2009; Abiola and James, 2010; Leelavathi and Rajalakshmi, 2013b). These compounds have the functional groups which correlate to the ones identified in the current study. It is difficult to tell which compounds have exactly participated in adsorption as well as corrosion inhibition, because FT-IR test is for identification of the functional groups only, and not for the molecular structure and identification of the specific compounds.

The optimal concentration of the investigated inhibitor at various temperatures is important to be determined. This is so because the application of any corrosion inhibitor must involve its working ability under a specific temperature and concentration of the medium. When comparing the optimal concentrations values (for the inhibitor investigated in both of the media), they seem to range from 60 to 80 v/v %, with a maximum inhibition efficiency of 71.67% in H_2SO_4 and 56.02 % in H_3PO_4. The low inhibition efficiency of the inhibitor in H_3PO_4 can be associated with the high dissolution kinetics of aluminium in H_3PO_4 medium, because high adsorption power was needed to overcome such dissolution as compared to when it was found in H_2SO_4 medium. In both of the media there is a little decrease in efficiency beyond the optimal concentration, this is due to the competition of the adsorbed species on the metal surface (Keera, 2003; Xing and Rankin, 2006). In corrosion inhibitor

studies the type of adsorption which has taken place is very important to be known. This is simply known through determining the model of adsorption using adsorption isotherms; together with thermodynamic and kinetic parameters. Various adsorption isotherms have been tested and the Langmuir adsorption isotherm has found to be the best by having the highest correlation coefficient values of approximately equal to 1. This isotherm is for determination of either chemical or physical adsorption (Yurt *et al.*, 2006; Prabhu and Rao, 2013). Therefore, through additional consideration of the kinetic and thermodynamic parameters which have been determined in this study, we can confirm that, physical adsorption is what took place in all cases of the media investigated.

Apart from all explanations given above, it is generally that; when inhibition efficiency decreases with the increase in temperatures, the tendency reveals the occurrence of physical adsorption. For chemical adsorption inhibition efficiency values increase with the increase in temperature (James and Akaranta, 2009; Obi-Egbedi *et al.*, 2012).

The surface profile analysis conducted this study revealed the inhibitor activeness by being adsorbed on the metal surface. Information concerning inhibitive properties of the *C. papaya* leaves extract obtained this study are the initial steps towards an attempt/journey of developing a commercialized corrosion inhibitor. This is so because every application needs specific abilities of inhibitor at various concentrations, temperature and the medium under such application (Rudy, 2002; Schmitt, 2013). Thus, formulating the inhibitor package from the plants' extracts may involve the addition of other materials to enhance its performance.

4.2 Conclusion

The corrosion inhibition ability of the *Carica papaya* extract in acidic media, which have been reported in this study and other investigations, revealed its moderate to high inhibition efficiency values. This proves that, *Carica papaya* extracts can be used to develop a corrosion inhibitor to be used in various applications such as acid pickling, descaling, electropolishing and oil well acidization.

4.3 Recommendations

The study of *Carica papaya* as a corrosion inhibitor of aluminium and its alloys can be done by considering other acids such as $HClO_4$ and HNO_3. Theoretical study can be employed in investigating the plant constituents (phytochemicals). Isolation and characterization of

phytochemicals then test for the active ones can also be employed in this study. An electrochemical measurement technique which involves potentiodynamic polarization and Electrochemical Impedance Spectroscopy (EIS) can be used in data collection instead of the weight loss method.

REFERENCES

Negm, N. A., Yousef, M. A. and Tawfik, S. M. (2013). Impact of synthesized and natural compounds in corrosion inhibition of carbon steel and aluminium in acidic media. *Recent Patents on Corrosion Science*. ***3*** (1): 58-68.

Aballe, A., Bethencourt, M., Botana, F. and Marcos, M. (2001). $CeCl_3$ and $LaCl_3$ binary solutions as environment-friendly corrosion inhibitors of AA5083 Al–Mg alloy in NaCl solutions. *Journal of Alloys and Compounds*. ***323***: 855-858.

Abd-El-Nabey, B., Abdel-Gaber, A., Elawady, G. and El-Housseind, S. (2012). Inhibitive action of some plant extracts on the alkaline corrosion of aluminum. *International Journal of electrochemical science. **7:*** 7823-7839.

Abiola, O. K. and James, A. (2010). The effects of *Aloe vera* extract on corrosion and kinetics of corrosion process of zinc in HCl solution. *Corrosion Science*. ***52*** (2): 661-664.

Ali, A. and Foaud, N. (2012). Inhibition of aluminum corrosion in hydrochloric acid solution using black mulberry extract. *Journal of Materials and Environmental Science*. ***3*** (5): 917-924.

Amin, M. A., Abd EI-Rehim, S. S., El-Sherbini, E. E., Hazzazi, O. A. and Abbas, M. N. (2009a). Polyacrylic acid as a corrosion inhibitor for aluminium in weakly alkaline solutions. Part I: Weight loss, polarization, impedance EFM and EDX studies. *Corrosion Science*. ***51*** (3): 658-667.

Amin, M. A., Mohsen, Q. and Hazzazi, O. A. (2009b). Synergistic effect of I^- ions on the corrosion inhibition of Al in 1.0 M phosphoric acid solutions by purine. *Materials Chemistry and Physics*. ***114*** (2): 908-914.

Ansari, A., Znini, M., Hamdani, I., Majidi, L., Bouyanzer, A. and Hammouti, B. (2013). Experimental and theoretical investigations anti-corrosive properties of Menthone on mild steel corrosion in hydrochloric acid. ***5*** (1): 81-94.

Arellanes-Lozada, P., Olivares-Xometl, O., Guzmán-Lucero, D., Likhanova, N. V., Domínguez-Aguilar, M. A., Lijanova, I. V. and Arce-Estrada, E. (2014). The inhibition of aluminum corrosion in sulfuric acid by poly (1-vinyl-3-alkyl-imidazolium hexafluorophosphate). *Materials*. ***7*** (8): 5711-5734.

Arockiasamy, P., Sheela, X., Thenmozhi, G., Franco, M., Sahayaraj, J. W. and Santhi, R. J. (2014). Evaluation of Corrosion Inhibition of Mild Steel in 1 M Hydrochloric Acid Solution by *Mollugo cerviana*. *International Journal of Corrosion*. ***2014***: 1-7

Avwiri, G. O. and Igho, F. (2003). Inhibitive action of *Vernonia amygdalina* on the corrosion of aluminium alloys in acidic media. *Materials Letters*. ***57*** (22): 3705-3711.

Ayeni, F., Madugu, I., Sukop, P., Ihom, A., Alabi, O., Okara, R. and Abdulwahab, M. (2012). Effect of Aqueous Extracts of Bitter Leaf Powder on the Corrosion Inhibition of Al-Si Alloy in 0.5 M Caustic Soda Solution. *Journal of Minerals and Materials Characterization and Engineering*. ***11*****:** 667-670.

Canini, A., Alesiani, D., D'Arcangelo, G. and Tagliatesta, P. (2007). Gas chromatography–mass spectrometry analysis of phenolic compounds from *Carica papaya* leaves. *Journal of Food Composition and Analysis*. ***20*** (7): 584-590.

Dariva, C. G. and Galio, A. F. (2014). Corrosion Inhibitors–Principles, Mechanisms and Applications. Science. *INTECH Open Access Book Publisher.* Rijeka, Croatia.

Ebenso, E., Alemu, H., Umoren, S. and Obot, I. (2008). Inhibition of mild steel corrosion in sulphuric acid using alizarin yellow GG dye and synergistic iodide additive. ***3*** (2008) : 1325-1339.

Eddy, N. O. (2009). Inhibitive and adsorption properties of ethanol extract of *Colocasia esculenta* leaves for the corrosion of mild steel in H_2SO_4. *International Journal of Physical Sciences*. ***4*** (4): 165-171.

Eddy, N. O., Momoh-Yahaya, H. and Oguzie, E. E. (2015). Theoretical and experimental studies on the corrosion inhibition potentials of some purines for aluminum in 0.1 M HCl. *Journal of Advanced Research*. ***6*** (2): 203-217.

El Maghraby, A. (2009). Corrosion Inhibition of Aluminum in Hydrochloric Acid Solution Using Potassium Iodate Inhibitor. *The Open Corrosion Journal* ***2*****:** 189-196.

Fouda, A., Abdallah, M., Ahmed, I. and Eissa, M. (2012). Corrosion inhibition of aluminum in 1M H_3PO_4 solutions by ethanolamines. *Arabian Journal of Chemistry*. ***5*** (3): 297-307.

Fouda, A., Abdallah, M. and Eissa, M. (2013). Corrosion inhibition of Aluminum in 1 M phosphoric acid solutions using some Chalcones derivatives and synergistic action with halide ions. *African Journal of Pure and Applied*. ***7*** (12): 394-404.

Hamdy, A. and El-Gendy, N. S. (2013). Thermodynamic, adsorption and electrochemical studies for corrosion inhibition of carbon steel by henna extract in acid medium. *Egyptian Journal of Petroleum*. ***22*** (1): 17-25.

Hamdy, A. S., El-Shenawy, E. and El-Bitar, T. (2006). Electrochemical impedance spectroscopy study of the corrosion behaviour of some niobium bearing stainless steels in 3.5% NaCl. *International Journal of Electrochemical Science*. ***1*** (4): 171-80.

Hassan, R. M. and Zaafarany, I. A. (2013). Kinetics of corrosion inhibition of aluminum in acidic media by water-soluble natural polymeric pectates as anionic polyelectrolyte inhibitors. *Materials*. ***6*** (6): 2436-2451.

James, A. and Akaranta, O. (2009). Corrosion inhibition of aluminium in 2.0 M Hydrochloric acid solution by the acetone extract of red onion Skin. *African Journal of Pure and Applied Chemistry*. ***3*** (12): 262-268.

Kavitha, N., Manjula, P. and Anandha, M. (2014). Syneristic effect of *C. papaya* leaves Extract-Zn^{+2} in Corrosion inhibition of Mild Steel in Aqueous Medium. *Research Journal of Chemical Sciences*. ***4*** (8): 88-93.

Keera, S. (2003). Inhibition of corrosion of carbon steel in acid solutions by tetratriethanolamine trioleiate. *Journal of Scientific and Industrial Research*. ***62*** (3): 188-192.

Kesavan, D., Gopiraman, M. and Sulochana, N. (2012). Green inhibitors for corrosion of metals: A review. *Chemical Science and Review Letters.* ***1*** (1): 1-8

Kini, A. U., Shetty, P., Shetty, D. S. and Isloor, A. M. (Ed.) (2011). Corrosion Inhibition of Al6061-SiC_p Composite in 0.5 M Hydrochloric Acid. *In: Proceedings of International Conference on Chemistry and Chemical Process*. ***10*** (2011): 127-132

Ladha, D., Naik, U. and Shah, N. (2013) Investigation of Cumin (*Cuminum Cyminum*) extract as an eco-friendly green corrosion inhibitor for pure Aluminium in Acid medium. ***4*** (5): 701-708.

Laouali, D. and Bénière, F. (2012). Evaluation of inhibitor efficiency on corrosion of the aluminium heart exchangers and radiators in central heating. *Journal of Materials and Environmental Science.* ***3*** (1): 34-39.

Lebrini, M., Robert, F. and Roos, C. (2013). Adsorption Properties and Inhibition of C38 Steel Corrosion in Hydrochloric Solution by Some Indole Derivates: Temperature Effect, Activation Energies, and Thermodynamics of Adsorption. *International Journal of Corrosion*. ***2013***: 1-13.

Leelavathi, S. and Rajalakshmi, R. (2013a). *Dodonaea viscosa* (L.) leaves extract as acid corrosion inhibitor for mild steel–a green approach. *Journal of Materials and Environmental Science.*. ***4*** (5): 625-638.

Leelavathi, S. and Rajalakshmi, R. (2013b). *Dodonaea viscosa* (L.) leaves extract as acid corrosion inhibitor for mild steel–a green approach. *Journal of Materials and Environmental Science*. ***4***: 625-638.

Li, X. and Deng, S. (2012). Inhibition effect of *Dendrocalamus brandisii* leaves extract on aluminum in HCl, H_3PO_4 solutions. *Corrosion Science*. ***65***: 299-308.

Loto, C. (2012). Electrode Potential Evaluation of Effect of Inhibitors on the Electrochemical Corrosion Behaviour of Mild Steel Reinforcement in Concrete in H_2SO_4. *Journal of Materials and Environmental Science.* ***3*** (1): 195-205.

Loto, C., Joseph, O., Loto, R. and Popoola, A. (2014). Corrosion Inhibitive Behaviour of *Camellia Sinensis* on Aluminium Alloy in H_2SO_4. *International Journal of Electrochemical Science*. ***9*** : 1221-1231.

Loto, C., Loto, R. and Popoola, A. (2011). Inhibition Effect of Extracts of *Carica Papaya* and *Camellia Sinensis* Leaves on the Corrosion of Duplex (α β) Brass in 1M Nitric acid. *International Journal of Electrochemical Science*. ***6*** : 4900-4914.

Mahendru Sr, P. and Mahindru, D. (2011). Protective Treatment of Aluminium and its Alloys. *Global Journal of Researches In Engineering*. ***11*** (3): 1-5.

Moutarlier, V., Gigandet, M., Normand, B. and Pagetti, J. (2005). EIS characterisation of anodic films formed on 2024 aluminium alloy, in sulphuric acid containing molybdate or permanganate species. *Corrosion Science*. ***47*** (4): 937-951.

Musa, A. Y. (2012a). Corrosion protection of Al alloys: Organic coatings and inhibitors. *INTECH Open Access Book Publisher*. Rijeka, Croatia. *pp*. 56-66

Musa, A. Y. (2012b). Corrosion protection of Al alloys: Organic coatings and inhibitors. *INTECH Open Access Book Publisher*. Rijeka, Croatia. *pp*. 52-55

Musa, A. Y., Mohamad, A. B., Kadhum, A. A. H. and Chee, E. P. (2011). Galvanic corrosion of aluminum alloy (Al 2024) and copper in 1.0 M nitric acid. *International Journal of Electrochemical Science.* ***6***: 5052-5065.

Nahlé, A., Abu-Abdoun, I. I. and Abdel-Rahman, I. (2012). Effect of temperature on the corrosion inhibition of trans-4-hydroxy-4′-stilbazole on mild steel in HCl solution. *International Journal of Corrosion*. ***2012***: 1-7.

Nakano, H., Oue, S., Taguchi, S., Kobayashi, S. and Horita, Z. (2012). Stress-corrosion cracking property of aluminum-magnesium alloy processed by equal-channel angular pressing. *International Journal of Corrosion*. ***2012***: 1-8.

Nwosu, O., Osarolube, E., Nnanna, L., Akoma, C. and Chigbu, T. (2014). Acidic Corrosion Inhibition of *Piper guineense* Seed Extract on Al Alloy. *American Journal of Materials Science*. ***4*** (4): 178-183.

Obi-Egbedi, N., Obot, I. and Umoren, S. (2012). *Spondias mombin* L. as a green corrosion inhibitor for aluminium in sulphuric acid: Correlation between inhibitive effect and electronic properties of extracts major constituents using density functional theory. *Arabian Journal of Chemistry*. ***5*** (3): 361-373.

Obot, I. and Obi-Egbedi, N. (2010). Theoretical study of benzimidazole and its derivatives and their potential activity as corrosion inhibitors. *Corrosion Science*. ***52*** (2): 657-660.

Obot, I., Umoren, S. and Obi-Egbedi, N. (2011). Corrosion inhibition and adsorption behaviour for aluminuim by extract of *Aningeria robusta* in HCl solution: synergistic effect of iodide ions. *Journal of Materials and Environmental Science*. ***2*** (1): 60-71.

Odewunmi, N., Umoren, S. and Gasem, Z. (2015). Watermelon waste products as green corrosion inhibitors for mild steel in HCl solution. *Journal of Environmental Chemical Engineering*. ***3*** (1): 286-296.

Oguzie, E. E. (2007). Corrosion inhibition of aluminium in acidic and alkaline media by Sansevieria trifasciata extract. *Corrosion Science*. ***49*** (3): 1527-1539.

Okafor, P. and Ebenso, E. (2007). Inhibitive action of *Carica papaya* extracts on the corrosion of mild steel in acidic media and their adsorption characteristics. *Pigment and Resin Technology*. ***36*** (3): 134-140.

Oki, M., Anawe, P. A. and Fasakin, J. (2015). Performance of Mild Steel in Nitric Acid/*Carica Papaya* Leaf Extracts Corrosion System. *Asian Journal of Applied Sciences*. ***3*** (1): 1-7.

Oya, Y., Kojima, Y. and Hara, N. (2013). Influence of Silicon on Intergranular Corrosion for Aluminum Alloys. *Materials Transactions*. ***54*** (7): 1200-1208.

Prabhu, D. (2013). Studies of Corrosion of Aluminium and 6063 Aluminium Alloy in Phosphoric Acid Medium. *International Journal of ChemTech Research*. ***5*** (6): 2690-2705.

Prabhu, D. and Rao, P. (2013). *Garcinia indica* as an environmentally safe corrosion inhibitor for aluminium in 0.5 M phosphoric acid. *International Journal of Corrosion*. ***2013***: 1-13.

Quraishi, M., Singh, A., Singh, V. K., Yadav, D. K. and Singh, A. K. (2010). Green approach to corrosion inhibition of mild steel in hydrochloric acid and sulphuric acid solutions by the extract of *Murraya koenigii* leaves. *Materials Chemistry and Physics*. ***122*** (1): 114-122.

Radojčić, I., Berković, K., Kovač, S. and Vorkapić-Furač, J. (2008). Natural honey and black radish juice as tin corrosion inhibitors. *Corrosion Science*. ***50*** (5): 1498-1504.

Rahim, A. A. and Kassim, J. (2008). Recent development of vegetal tannins in corrosion protection of iron and steel. *Recent Patents on Materials Science*. ***1*** (3): 223-231.

Raja, P. B. and Sethuraman, M. G. (2008). Natural products as corrosion inhibitor for metals in corrosive media—a review. *Materials Letters*. ***62*** (1): 113-116.

Rajalakshmi, R., Subhashini, S., Leelavathi, S. and Geethanjali, R. (2010). Study of the inhibitive action of bakery waste for corrosion of mild steel in acid medium. *Journal of Nepal Chemical Society*. ***25:*** 29-36.

Rajendran, S., Thangavelu, C. and Annamalai, G. (2012). Inhibition of corrosion of aluminium in alkaline medium by succinic acid in conjunction with zinc sulphate and diethylene triamine penta (Methylene phosphonic acid). *Journal of Chemical and Pharmaceutical Research*. ***4*** (11): 4836-4844

Rani, B. and Basu, B. B. J. (2011). Green inhibitors for corrosion protection of metals and alloys: An overview. *International Journal of Corrosion*. ***2012***: 1-15.

Rudy, S. F. (2002). Pickling and acid dipping. *Metal Finishing*. ***100*****:** 173-179.

Sangeetha, M., Rajendran, S., Muthumegala, T. and Krishnaveni, A. (2011). Green corrosion inhibitors–An overview. *Zastita Materijala*. ***52*** (1): 3-19.

Sangeetha, M., Rajendran, S., Sathiyabama, J. and Prabhakar, P. (2012). Eco-friendly extract of Banana peel as corrosion inhibitor for carbon steel in sea water. *Journal of Natural Products and Plant Resources*. ***2*** (5): 601-610.

Schmitt, G. (2009). Global needs for knowledge dissemination, research, and development in materials deterioration and corrosion control. The World Corrosion Organization. New York, NY. 44 pp.

Schmitt, G. (2013). Application of inhibitors for acid media: report prepared for the european federation of corrosion working party on inhibitors. *British Corrosion Journal*. ***19*** (4): 165-176.

Shivakumar, S. and Mohana, K. (2013). Corrosion Behaviour and Adsorption Thermodynamics of Some Schiff Bases on Mild Steel Corrosion in Industrial Water Medium. *International Journal of Corrosion*. ***2013***: 1-13.

Singh, A., Ebenso, E. E. and Quraishi, M. (2012). Corrosion Inhibition of carbon steel in HCl solution by some plant extracts. *International Journal of Corrosion*. ***2012***: 1-20.

Son, I., Nakano, H., Oue, S., Kobayashi, S., Fukushima, H. and Horita, Z. (2012). Effect of equal-channel angular pressing on pitting corrosion of pure aluminum. *International Journal of Corrosion*. ***2012***: 1-9.

Umoren, S. (2009). Synergistic influence of Gum Arabic and iodide ion on the corrosion inhibition of aluminium in alkaline medium. *Portugaliae Electrochimica Acta*. ***27*** (5): 565-577.

Umoren, S., Ebenso, E. and Ogbobe, O. (2009). Synergistic effect of halide ions and polyethylene glycol on the corrosion inhibition of aluminium in alkaline medium. *Journal of Applied Polymer Science*. ***113*** (6): 3533-3543.

Xing, R. and Rankin, S. E. (2006). Three-stage multilayer formation kinetics during adsorption of an anionic fluorinated surfactant onto germanium. 1. Concentration effect. *The Journal of Physical Chemistry B*. ***110*** (1): 295-304.

Xiong, Y., Brown, B., Kinsella, B., Nesic, S. and Pailleret, A. (2013). AFM Studies of the Adhesion Properties of Surfactant Corrosion Inhibitor Films. *CORROSION* ***2013***: 1-22

Yadav, M., Sinha, R., Sarkar, T., Bahadur, I. and Ebenso, E. (2015). Application of new isonicotinamides as a corrosion inhibitor on mild steel in acidic medium: Electrochemical, SEM, EDX, AFM and DFT investigations. *Journal of Molecular Liquids*. ***212:*** 686-698

Yiase, S. G., Adejo, S. O., Tyohemba, T. G., Ahile, U. J. and Gbertyo, J. A. (2014). Thermodynamic, Kinetic and Adsorptive Parameters of Corrosion Inhibition of Aluminium Using Sorghum bicolor Leaf Extract in H_2SO_4. ***1*** (2): 38-46.

Yurt, A., Ulutas, S. and Dal, H. (2006). Electrochemical and theoretical investigation on the corrosion of aluminium in acidic solution containing some Schiff bases. *Applied Surface Science*. ***253*** (2): 919-925.

Zaferani, S. H., Sharifi, M., Zaarei, D. and Shishesaz, M. R. (2013). Application of eco-friendly products as corrosion inhibitors for metals in acid pickling processes–A review. *Journal of Environmental Chemical Engineering*. ***1*** (4): 652-657.

APPENDICES

Appendix 1: Tables with the weight loss results, calculations of inhibition efficiency, corrosion rate, adsorption isotherms, thermodynamic and kinetic parameters (for the first objective)

(i) Tables show weight loss measurement results; experiments were repeated three times at each temperature and the average weight loss were calculated.

1st Experiment at 30^0C

Conc. (v/v %)	W-1	W-2	Weight loss-1	W-1	W-2	Weight loss-2	W-1	W-2	Weight loss-3	Average Weight loss
BLANK	1.3769	1.3650	0.0119	1.3778	1.3655	0.0123	1.3125	1.3007	0.0118	0.0120
20	1.1377	1.1327	0.0050	1.1377	1.1327	0.0050	1.2747	1.2699	0.0048	0.0049
40	1.1135	1.1096	0.0039	1.1135	1.1096	0.0039	1.3535	1.3498	0.0037	0.0038
60	1.0768	1.0733	0.0035	1.0768	1.0733	0.0035	1.347	1.3437	0.0033	0.0034
80	1.2755	1.2720	0.0035	1.2755	1.2720	0.0035	1.3001	1.2968	0.0033	0.0034
100	1.3405	1.3369	0.0036	1.3405	1.3369	0.0036	1.3059	1.3023	0.0036	0.0036

2nd Experiment at 40^0C

Conc. (v/v %)	W-1	W-2	Weight loss-1	W-1	W-2	Weight loss-2	W-1	W-2	Weight loss-3	Average weight loss
BLANK	1.354	1.3182	0.0358	1.314	1.2777	0.0363	1.0902	1.0546	0.0356	0.0359
20	1.342	1.327	0.0150	1.3183	1.3031	0.0152	1.3057	1.2908	0.0149	0.0150
40	1.3134	1.3002	0.0132	1.395	1.3821	0.0129	1.3633	1.3504	0.0129	0.0130
60	1.3393	1.3271	0.0122	1.3172	1.3050	0.0122	1.1221	1.1099	0.0122	0.0122
80	1.3088	1.297	0.0118	1.2852	1.2733	0.0119	1.0585	1.0468	0.0117	0.0118
100	1.2856	1.2731	0.0125	1.2685	1.2558	0.0127	1.263	1.2505	0.0125	0.0126

3rd Experiment at 50^0C

Conc. (v/v %)	W-1	W-2	Weight loss-1	W-1	W-2	Weight loss-2	W-1	W-2	Weight loss-3	Average weight loss
BLANK	1.3013	1.2159	0.0854	1.3172	1.2202	0.0857	1.2956	1.2099	0.0857	0.0856
20	1.3155	1.2728	0.0427	1.3059	1.2514	0.0428	1.3634	1.3205	0.0429	0.0428
40	1.2925	1.2548	0.0377	1.2942	1.2997	0.0378	1.3734	1.3355	0.0379	0.0378
60	1.34	1.3047	0.0353	1.3375	1.3606	0.0354	1.3197	1.2843	0.0354	0.0354
80	1.3143	1.2784	0.0359	1.3960	1.1850	0.0360	1.3712	1.3351	0.0361	0.0360
100	1.3383	1.2999	0.0384	1.2210	1.3364	0.0384	1.3013	1.2629	0.0384	0.0384

(ii) Calculations involve In CR and ln (CR/T) at 30^0C, 40^0C, 50^0 C

		30^0C		
Average weight loss	CR	ln CR	CR/T	ln(CR/T)
0.012	0.000 055 80	-9.793 67	1.8417E-07	-15.507 41
0.0049	0.000 022 79	-10.689 34	7.52028E-08	-16.403 08
0.0038	0.000 017 67	-10.943 58	5.83206E-08	-16.657 31
0.0034	0.000 015 81	-11.054 80	5.21816E-08	-16.768 54
0.0034	0.000 015 81	-11.054 80	5.21816E-08	-16.768 54
0.0036	0.000 016 74	-10.997 5	5.52511E-08	-16.711 38

40^0C				
Average weight loss	CR	ln CR	CR/T	ln (CR/T)
0.0359	0.000 166 95	-8.697 84	5.334E-07	-14.444 05
0.015	0.000 069 75	-9.570 53	2.229E-07	-15.316 73
0.013	0.000 060 45	-9.713 63	1.931E-07	-15.459 83
0.0122	0.000 056 73	-9.777 14	1.813E-07	-15.523 35
0.0118	0.000 054 87	-9.810 48	1.753E-07	-15.556 68
0.0126	0.000 058 59	-9.744 88	1.872E-07	-15.491 09

50^0C				
Average weight loss	CR	ln CR	CR/T	ln (CR/T)
0.0856	0.000 398 07	-7.828 89	1.2324E-06	-13.606 55
0.0428	0.000 199 03	-8.522 04	6.162E-07	-14.299 69
0.0378	0.000 175 78	-8.646 27	5.44214E-07	-14.423 92
0.0354	0.000 164 62	-8.711 87	5.09661E-07	-14.489 52
0.036	0.000 167 41	-8.695 06	5.18299E-07	-14.472 71
0.0384	0.000 178 57	-8.630 52	5.52853E-07	-14.408 17

(iii) A table which shows the values used for adsorption isotherm test and Gibbs energy at each temperature

1st Experiment at 30^0 C

C	I.E %	q	ln [q/(1-q)c	Log q	Log C	Log [q/(1-q)]	c/q	Gibbs energy
20	59.17	0.5917	-2.624 73	-0.227 90	1.301 03	0.161 122 189	33.800 91	-3.51
40	68.33	0.6833	-2.919 90	-0.165 39	1.602 06	0.333 9633 57	58.539 44	-2.76
60	71.67	0.7167	-3.166 19	-0.144 66	1.778 15	0.403 090 83	83.717 04	-2.14
80	71.67	0.7167	-3.453 88	-0.144 66	1.903 09	0.403 090 83	111.62 27	-1.42
100	70	0.7	-3.757 87	-0.154 90	2.000 00	0.367 976 7 85	142.85 71	-0.65

2nd Experiment at 40^0C

C	I.E%	q	ln [q/(1-q)c	Log q	Log C	Log [q/(1-q)]	c/q	Gibbs energy
20	58.32	0.5832	-2.659 81	-0.234 18	1.301 03	0.145 889 81	34.293 55	-3.53
40	63.88	0.6388	-3.118 72	-0.194 64	1.602 06	0.247 617 17	62.617 41	-2.34
60	65.98	0.6598	-3.431 94	-0.180 59	1.778 15	0.287 678	90.936 65	-1.52
80	67	0.67	-3.673 84	-0.173 93	1.903 09	0.307 560 86	119.403	-0.89
100	65.9	0.659	-3.946 33	-0.181 11	2.000 00	0.286 131 04	151.7451	-0.18

3rd Experiment at 50^0C

C	I.E %	q	ln [q /(1-q) c	Log q	Log C	Log [q/(1-q)]	c/q	Gibbs energy
20	50	0.5	-2.995 73	-0.301 03	1.301 03	0	40	-2.74
40	55.84	0.5584	-3.454 21	-0.253 05	1.602 06	0.101 916 345	71.633 24	-1.51
60	58.64	0.5864	-3.745 24	-0.231 81	1.778 15	0.151 613 432	102.3192	-0.73
80	57.94	0.5794	-4.061 72	-0.237 02	1.903 09	0.139 109 223	138.0739	0.12
100	55.14	0.5514	-4.398 84	-0.258 53	2.000 00	0.089 607 493	181.3565	1.03

(iv) The table shows calculations of enthalpy of activation, activation energy, entropy and heats of adsorption

Conc. (v/v %)	Slope-1	Ea	Slope-2	ΔH_a°	Inter	Entropy	S-Q_{ads}	Qads (KJ/mol)
Blank	9623	80.01	9310	77.40	-15.25	-70.75		
20	10606	88.18	10293	85.58	-17.57	-51.46	781.3	14.96
40	11246	93.50	10394	86.42	-19.44	-35.92	1132	21.67
60	11472	95.38	11159	92.78	-20.08	-30.59	1228	23.51
80	11550	96.03	11237	93.42	-20.33	-28.52	1287	24.64
100	11587	96.33	11274	93.73	-20.51	-27.02	1358	26.00

Appendix 2: Tables with weight loss results, calculations of inhibition efficiency, corrosion rate, adsorption isotherms, thermodynamic and kinetic parameters. (for the second objective)

(i) Tables show weight loss measurement results; experiments were repeated three times at each temperature and the average weight loss were calculated.

					30 C					
C (v/v %)	W-1	W-2	Weight loss-1	W-1	W-2	Weight loss-2	W-1	W-2	Weight loss-3	Average weight loss
Blank	1.3201	1.2502	0.0699	1.3289	1.2593	0.0696	1.2982	1.2284	0.0698	0.0698
20	1.3775	1.3384	0.0391	1.3025	1.2635	0.039	1.3902	1.351	0.0392	0.0391
40	1.3854	1.3520	0.0334	1.349	1.3156	0.0334	1.3308	1.2973	0.0335	0.0334
60	1.3311	1.2995	0.0316	1.3238	1.2923	0.0315	1.2865	1.2548	0.0317	0.0316
80	1.3809	1.3502	0.0307	1.3489	1.3182	0.0307	1.3294	1.2987	0.0307	0.0307
100	1.3115	1.2807	0.0308	1.2588	1.2281	0.0307	1.3677	1.3368	0.0309	0.0308

Conc (v/v%)					40 C					
	W-1	W-2	Weight loss-1	W-1	W-2	Weight loss-2	W-1	W-2	Weight loss-3	Average weight loss
Blank	1.2988	1.1285	0.1703	1.2498	1.0792	0.1706	1.1387	0.9683	0.1704	0.1704
20	1.3041	1.2053	0.0988	1.3102	1.2114	0.0988	1.1275	1.0287	0.0988	0.0988
40	1.3142	1.2217	0.0925	1.3312	1.2387	0.0925	1.1184	1.0259	0.0925	0.0925
60	1.3211	1.2341	0.087	1.2334	1.1463	0.0871	1.3011	1.2141	0.087	0.0870
80	1.3108	1.2253	0.0855	1.2527	1.1671	0.0856	1.221	1.1355	0.0855	0.0855
100	1.2995	1.2129	0.0866	1.2679	1.1812	0.0867	1.2324	1.1458	0.0866	0.0866

Conc. (v/v %)					50 C					
	W-1	W-2	Weight loss-1	W-1	W-2	Weight loss-2	W-1	W-2	Weight loss-3	Average weight loss
BLANK	1.23	0.8808	0.3492	1.3132	0.9641	0.3491	1.1876	0.8385	0.3491	0.3491
20	1.3332	1.1139	0.2193	1.2887	1.0698	0.2189	1.334	1.115	0.219	0.2191
40	1.2999	1.089	0.2109	1.1989	0.9884	0.2105	1.2312	1.0205	0.2107	0.2107
60	1.2974	1.0947	0.2027	1.2795	1.0772	0.2023	1.2618	1.0594	0.2024	0.2025
80	1.2829	1.0764	0.2065	1.3215	1.1154	0.2061	1.2813	1.075	0.2063	0.2063
100	1.1245	0.9175	0.207	1.3308	1.1237	0.2071	1.3017	1.0947	0.207	0.2070

(ii) Calculations involve In CR and ln (CR/T) at 30^0C, 40^0C, 50^0 C

C	303 K	CR	ln CR	ln CR/T	1/T
Blank	0.0698	0.000 324 59	-8.032 95	-13.746 68	0.003 300 33
20	0.0391	0.000 181 83	-8.612 46	-14.326 19	0.003 300 33
40	0.0334	0.000 155 32	-8.770 02	-14.483 76	0.003 300 33
60	0.0316	0.000 146 95	-8.825 42	-14.539 16	0.003 300 33
80	0.0307	0.000 142 76	-8.854 32	-14.568 05	0.003 300 33
100	0.0308	0.000 143 23	-8.851 06	-14.564 80	0.003 300 33

C	313K	CR	ln CR	ln CR/T	1/T
Blank	0.1704	0.000 792 41	-7.140 43	-12.886 63	0.003 194 89
20	0.0988	0.000 459 45	-7.685 48	-13.431 68	0.003 194 89
40	0.0925	0.000 430 15	-7.751 37	-13.497 57	0.003 194 89
60	0.0870	0.000 404 58	-7.812 67	-13.558 87	0.003 194 89
80	0.0855	0.000 397 60	-7.830 06	-13.576 27	0.003 194 89
100	0.0866	0.000 402 72	-7.817 28	-13.563 48	0.003 194 89

C	323	CR	ln CR	ln CR/T	1/T
Blank	0.3491	0.001 623 42	-6.423 22	-12.200 87	0.003 095 98
20	0.2191	0.001 018 88	-6.889 05	-12.666 70	0.003 095 98
40	0.2107	0.000 979 82	-6.928 14	-12.705 80	0.003 095 98
60	0.2025	0.000 941 69	-6.967 84	-12.745 49	0.003 095 98
80	0.2063	0.000 959 36	-6.949 25	-12.726 90	0.003 095 98
100	0.2070	0.000 962 61	-6.945 86	-12.723 51	0.003 095 98

(iii) A table which shows the values used for adsorption isotherm test and Gibbs energy at each temperature.

	TEMP.							
C	303K (I.E %)	q	Ln [q/(1-q)c]	Log q	Log c	Log [q/(1-q)]	c/q	Gibbs (kJ/mol)
20	43.98	0.4398	-3.237 71	-0.356 74	1.301 03	-0.105 09	45.475 22	-1.96
40	52.15	0.5215	-3.602 83	-0.282 75	1.602 06	0.037 37	76.701 82	-1.04
60	54.73	0.5473	-3.904 58	-0.261 77	1.778 15	0.082 41	109.629 09	-0.28
80	56.02	0.5602	-4.140 05	-0.251 66	1.903 09	0.105 09	142.806 14	0.31
100	55.87	0.5587	-4.369 28	-0.252 82	2.000 00	0.102 44	178.986 93	0.89

C	313K (I.E %)	q	ln [q/(1-q)c]	Log q	Log c	Log [q/(1-q)]	c/q	Gibbs (kJ/mol)
20	42.02	0.4202	-3.317 68	-0.376 54	1.301 03	-0.139 82	47.596 38	-1.82
40	45.72	0.4572	-3.860 50	-0.339 89	1.602 06	-0.074 53	87.489 06	-0.41
60	48.94	0.4894	-4.136 75	-0.310 34	1.778 15	-0.018 42	122.599 10	0.31
80	49.82	0.4982	-4.389 23	-0.302 60	1.903 09	-0.003 13	160.578 08	0.97
100	49.18	0.4918	-4.637 97	-0.308 21	2.000 00	-0.014 25	203.334 69	1.62

C	323K (I.E %)	q	ln [q/(1-q)c]	Log q	Log c	Log [q/(1-q)]	c/q	Gibbs (kJ/mol)
20	37.24	0.3724	-3.517 67	-0.428 99	1.301 03	-0.226 67	53.705 69	-1.34
40	39.64	0.3964	-4.109 37	-0.401 87	1.602 06	-0.182 62	100.908 17	0.25
60	41.99	0.4199	-4.417 53	-0.376 85	1.778 15	-0.140 36	142.891 16	1.08
80	40.91	0.4091	-4.749 71	-0.388 17	1.903 09	-0.159 68	195.551 21	1.97
100	40.7	0.407	-4.981 55	-0.390 41	2.000 00	-0.163 46	245.700 25	2.59

(iv) The table shows calculations of enthalpy of activation, activation energy, entropy and heats of adsorption.

C	Slope-1	ΔH_a°	Slope-2	Ea	Inter.	Entropy	S-Q_{ads}	Q_{ads} (kJ/mol)
Blank	7884	65.55	7571	62.95	11.26	-103.92		
20	8437	70.15	8125	67.55	12.5	-93.62	592	11.34
40	9020	74.99	8708	72.40	14.28	-78.82	1076	20.60
60	9096	75.62	8783	73.02	14.47	-77.24	1089	20.85
80	9327	77.54	9014	74.94	15.19	-71.25	1293	24.76
100	9328	77.55	9016	74.96	15.21	-71.08	1299	24.87

Note

W-1= Initial weight

W-2= Final weight

Weight loss-1, 2 & 3 are the weights lost at the same temperature because each experiment was done three times

Average weight loss= the average of Weight loss-1, Weight loss-2 and Weight loss-3

C= Concentration

Inter. = Intercept used in calculations of entropy

Slope-1= Slope used in calculations of activation energy

E_a = Activation energy

Slope-2= Slope used in calculations for enthalpy of activation

ΔH_a^o = Entropy of activation

S-Q_{ads}= Slopes used in calculations of heats of adsorption

Q_{ads}= Heat of adsorption

The following are the Formulas on determination of adsorption isotherms, and calculations of kinetic and thermodynamic parameters.

Equations used for testing adsorption isotherms by plotting graphs (For both objectives).

(i) Langmuir adsorption isotherm

$$\frac{C}{\theta} versus C$$

The equation used

$$\frac{C}{\theta} = \frac{1}{K} + C$$

(ii) Temkin adsorption isotherm

$$\theta versus \log C$$

Apply natural logarithm both sides and then express it in log base 10

$$\exp(-2a\theta) = KC$$

$$\theta = -\frac{1}{2a}(\ln K + \ln C)$$

$$\theta = -\frac{1.1515 logC}{a} - \frac{1.1515 logK}{a}$$

iii) Frumkin adsorption isotherm

$$\ln\left[\frac{\theta}{C(1-\theta)}\right] vesrus\theta$$

The equation below was used

$$\left(\frac{\theta}{1-\theta}\right)\exp(-2a\theta) = KC$$

Apply natural logarithm both sides to get equation used in plotting graphs

$$\ln\left(\frac{\theta}{C(1-\theta)}\right) = 2a\theta + K$$

(iv) Freundlich adsorption Isotherm

$$LogCversusLog\theta$$

The equation below was used

$$\log\theta = \log K + n\log C$$

Note:

Ɵ = q= Degree of surface

Appendix 3: Graphs for adsorption isotherms, and calculations of kinetic and thermodynamic parameters (for the first objective).

(i) Graphs for adsorption isotherm at 303 K, 313K and 323K

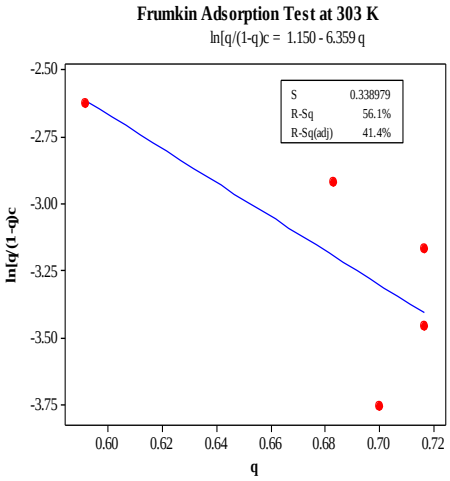

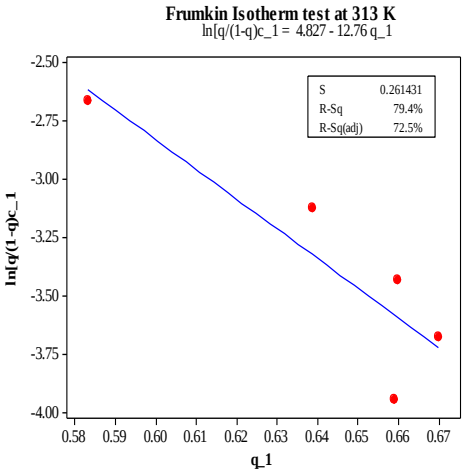

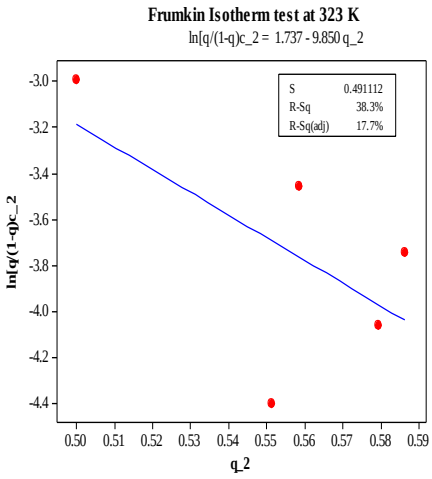

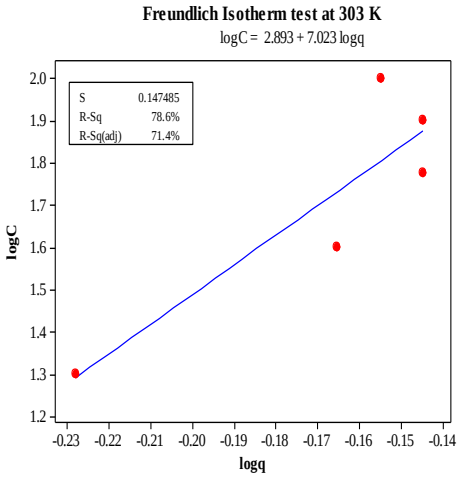

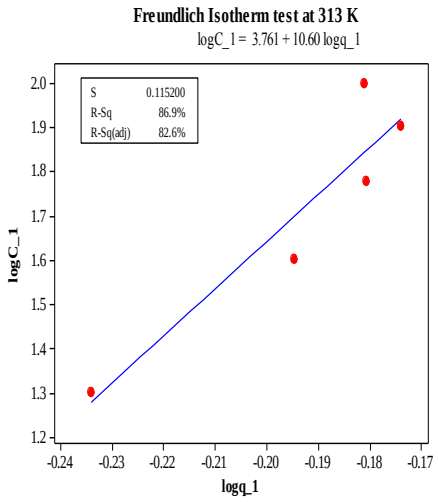
Freundlich Isotherm test at 313 K
logC_1 = 3.761 + 10.60 logq_1
S 0.115200
R-Sq 86.9%
R-Sq(adj) 82.6%
logC_1
logq_1

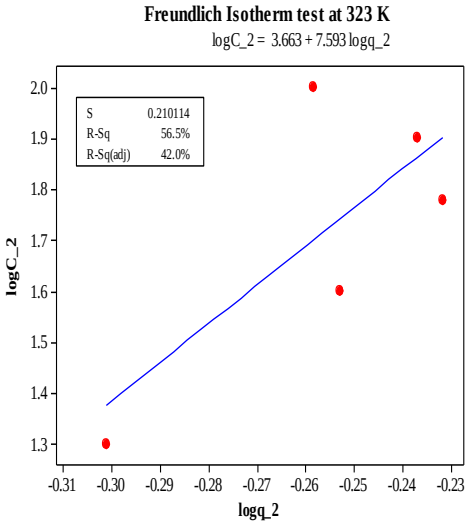
Freundlich Isotherm test at 323 K
logC_2 = 3.663 + 7.593 logq_2
S 0.210114
R-Sq 56.5%
R-Sq(adj) 42.0%
logC_2
logq_2

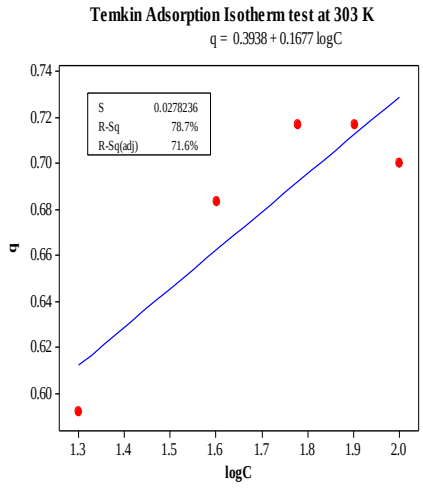
Temkin Adsorption Isotherm test at 303 K
q = 0.3938 + 0.1677 logC
S 0.0278236
R-Sq 78.7%
R-Sq(adj) 71.6%
q
logC

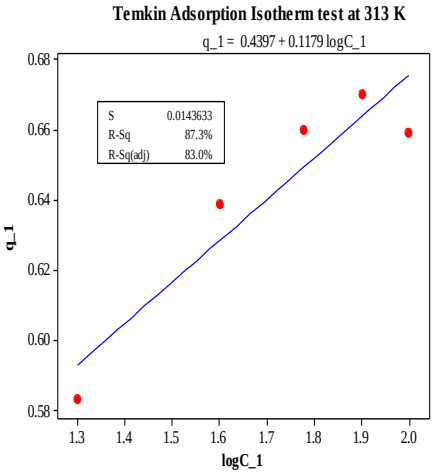
Temkin Adsorption Isotherm test at 313 K
q_1 = 0.4397 + 0.1179 logC_1
S 0.0143633
R-Sq 87.3%
R-Sq(adj) 83.0%
q_1
logC_1

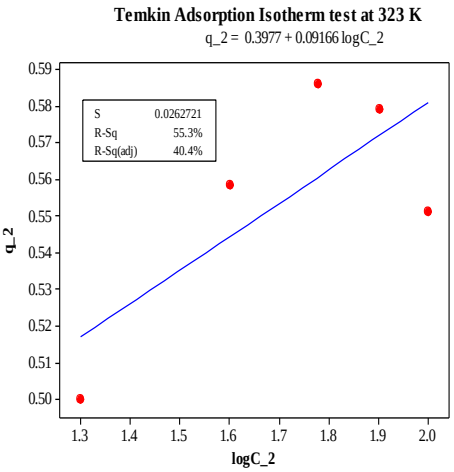
Temkin Adsorption Isotherm test at 323 K
q_2 = 0.3977 + 0.09166 logC_2
S 0.0262721
R-Sq 55.3%
R-Sq(adj) 40.4%
q_2
logC_2

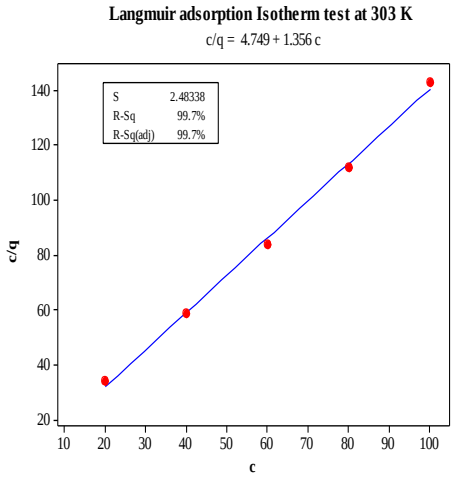
Langmuir adsorption Isotherm test at 303 K
c/q = 4.749 + 1.356 c
S 2.48338
R-Sq 99.7%
R-Sq(adj) 99.7%
c/q
c

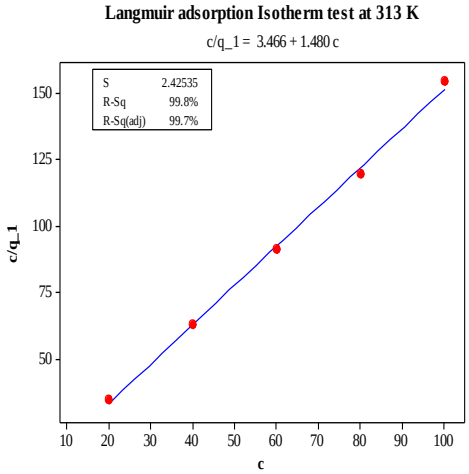
Langmuir adsorption Isotherm test at 313 K
c/q_1 = 3.466 + 1.480 c
S 2.42535
R-Sq 99.8%
R-Sq(adj) 99.7%
c/q_1
c

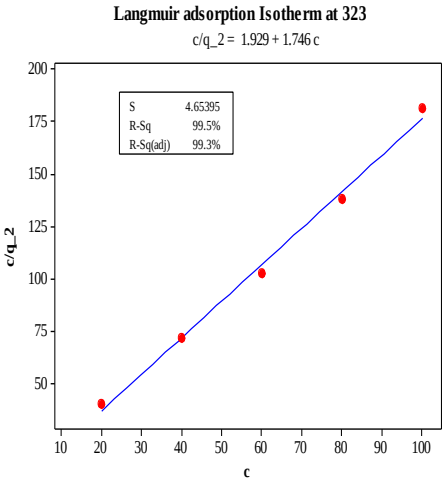
Langmuir adsorption Isotherm at 323
c/q_2 = 1.929 + 1.746 c
S 4.65395
R-Sq 99.5%
R-Sq(adj) 99.3%
c/q_2
c

(ii) Activation energy

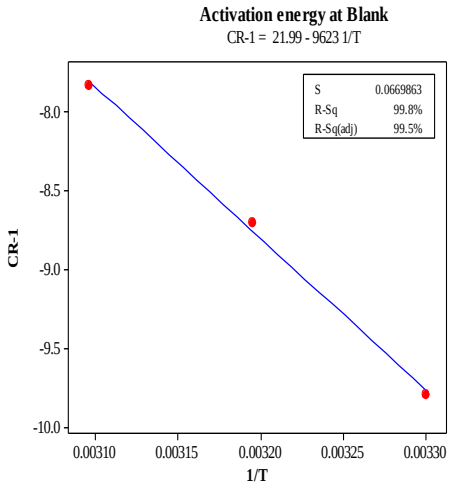

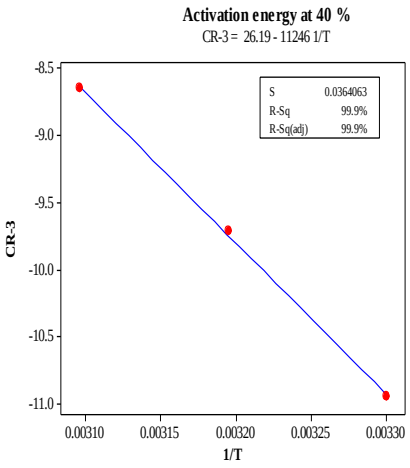

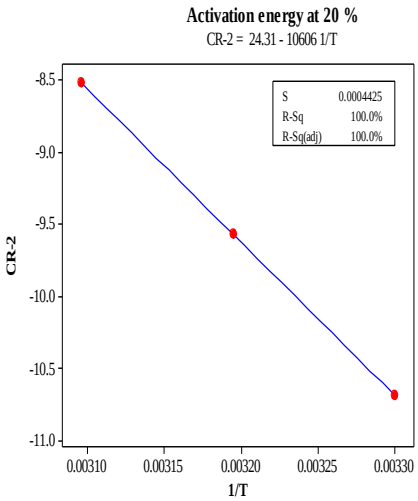

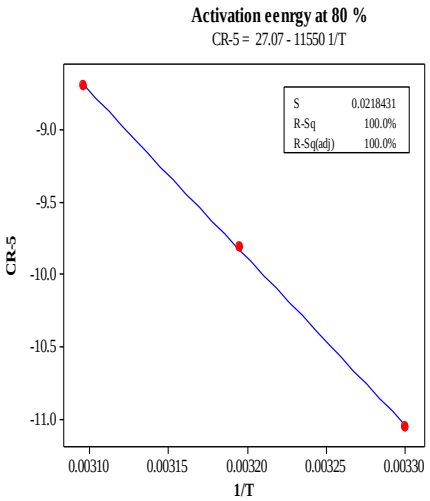

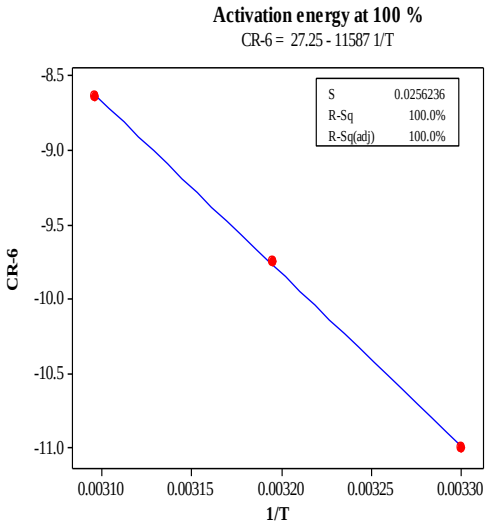

(iii) Enthalpy of activation

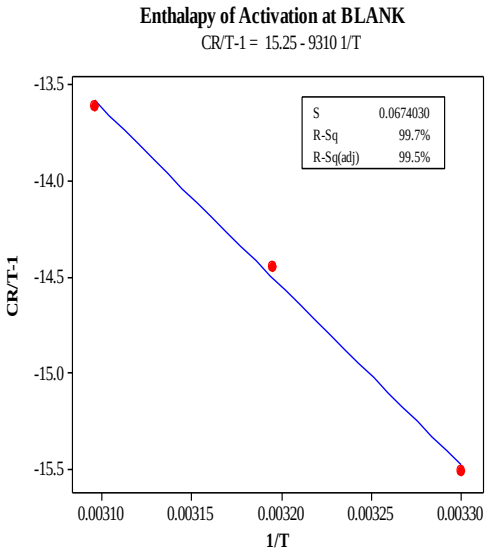

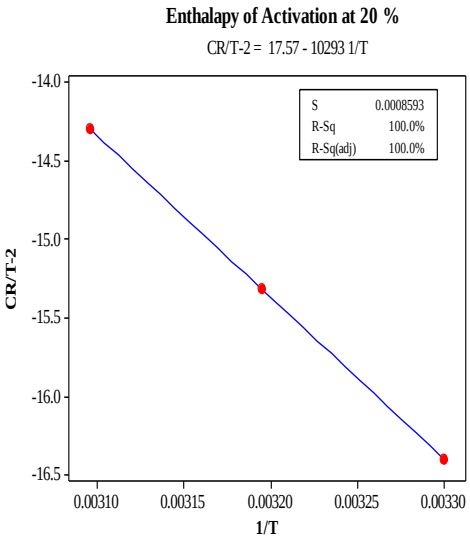

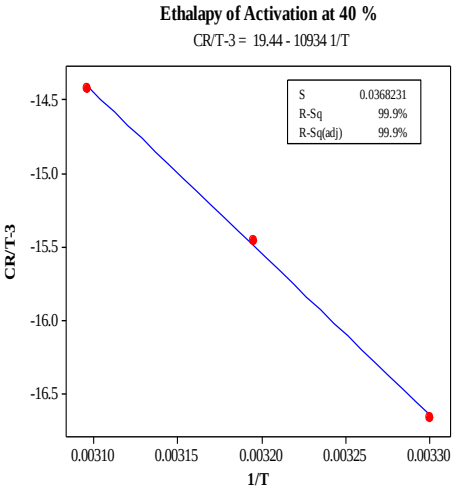
Ethalapy of Activation at 40 %
CR/T-3 = 19.44 - 10934 1/T
S 0.0368231
R-Sq 99.9%
R-Sq(adj) 99.9%
CR/T-3
-14.5
-15.0
-15.5
-16.0
-16.5
0.00310
0.00315
0.00320
0.00325
0.00330
1/T

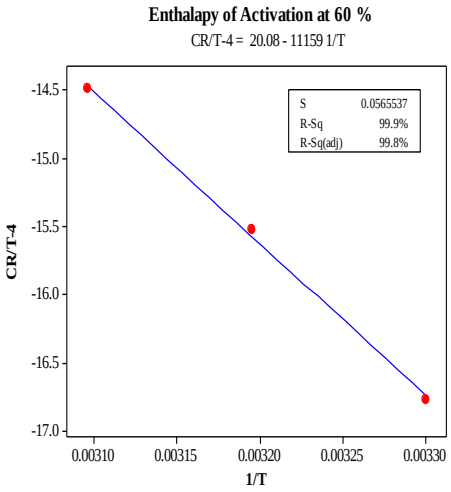
Enthalapy of Activation at 60 %
CR/T-4 = 20.08 - 11159 1/T
S 0.0565537
R-Sq 99.9%
R-Sq(adj) 99.8%
CR/T-4
-14.5
-15.0
-15.5
-16.0
-16.5
-17.0
0.00310
0.00315
0.00320
0.00325
0.00330
1/T

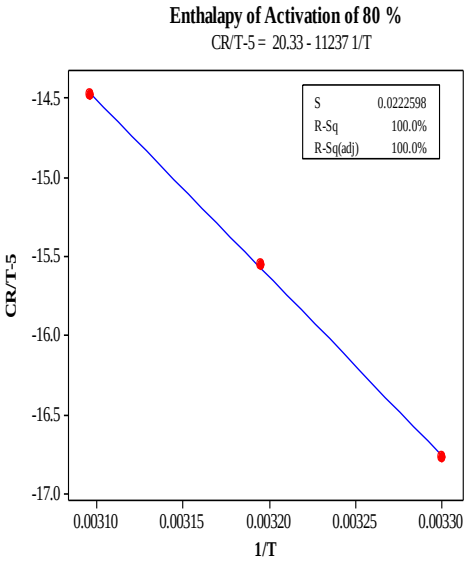
Enthalapy of Activation of 80 %
CR/T-5 = 20.33 - 11237 1/T
S 0.0222598
R-Sq 100.0%
R-Sq(adj) 100.0%
CR/T-5
-14.5
-15.0
-15.5
-16.0
-16.5
-17.0
0.00310
0.00315
0.00320
0.00325
0.00330
1/T

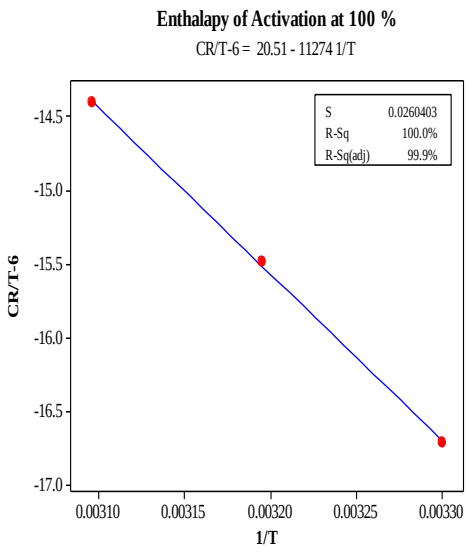
Enthalapy of Activation at 100 %
CR/T-6 = 20.51 - 11274 1/T
S 0.0260403
R-Sq 100.0%
R-Sq(adj) 99.9%
CR/T-6
-14.5
-15.0
-15.5
-16.0
-16.5
-17.0
0.00310
0.00315
0.00320
0.00325
0.00330
1/T

(iv) Heats of adsorption

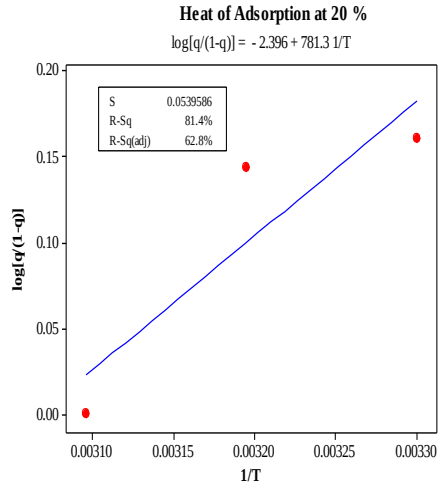

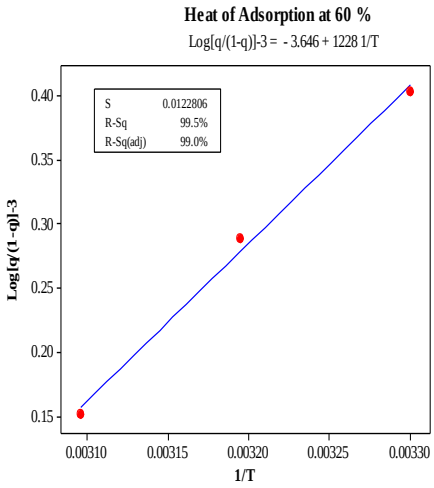

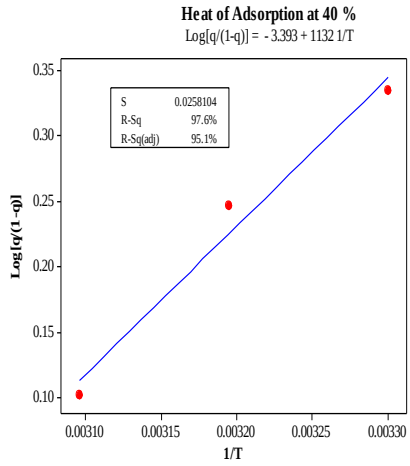

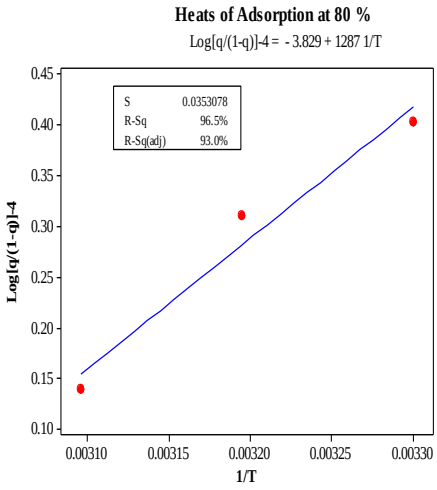

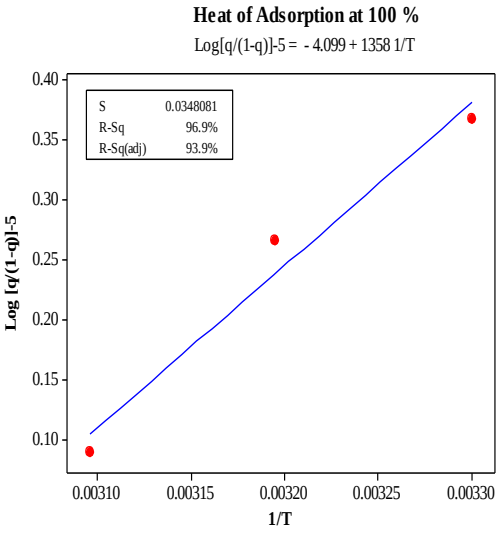

Appendix 4: Graphs for adsorption isotherms, and calculations of kinetic and thermodynamic parameters (for the second objective).

(i) Adsorption isotherms

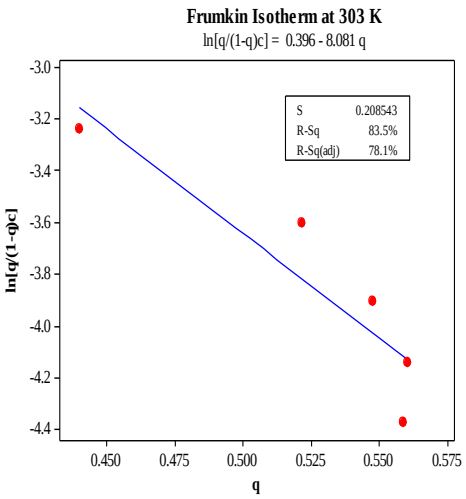

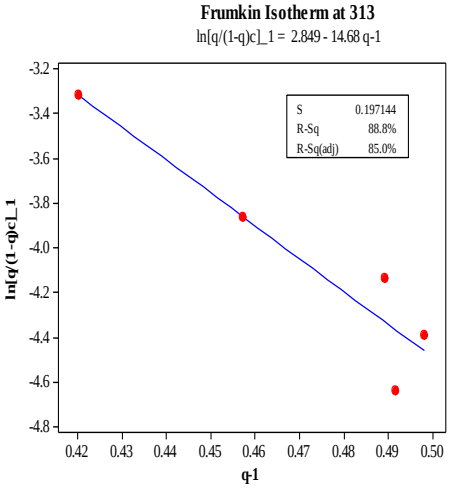

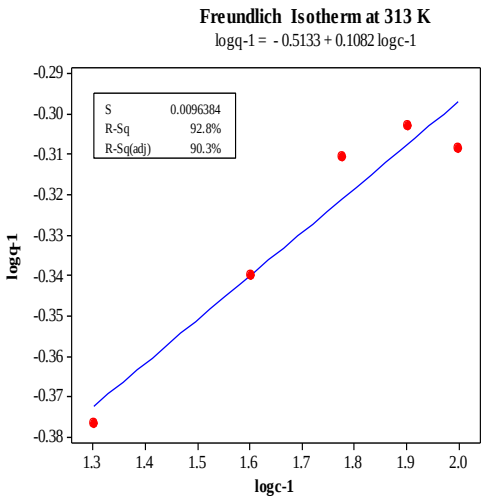
Freundlich Isotherm at 313 K
logq-1 = - 0.5133 + 0.1082 logc-1
S 0.0096384
R-Sq 92.8%
R-Sq(adj) 90.3%
logq-1
logc-1

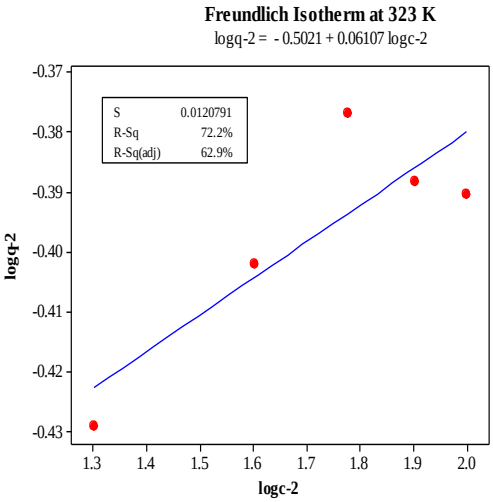
Freundlich Isotherm at 323 K
logq-2 = - 0.5021 + 0.06107 logc-2
S 0.0120791
R-Sq 72.2%
R-Sq(adj) 62.9%
logq-2
logc-2

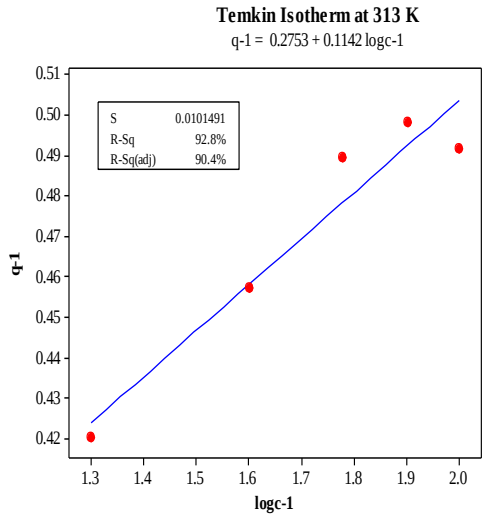
Temkin Isotherm at 313 K
q-1 = 0.2753 + 0.1142 logc-1
S 0.0101491
R-Sq 92.8%
R-Sq(adj) 90.4%
q-1
logc-1

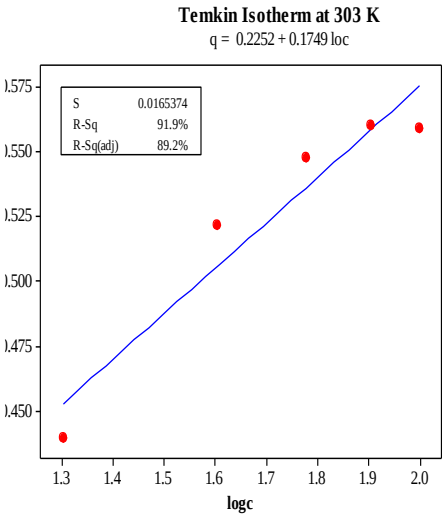
Temkin Isotherm at 303 K
q = 0.2252 + 0.1749 loc
S 0.0165374
R-Sq 91.9%
R-Sq(adj) 89.2%
logc

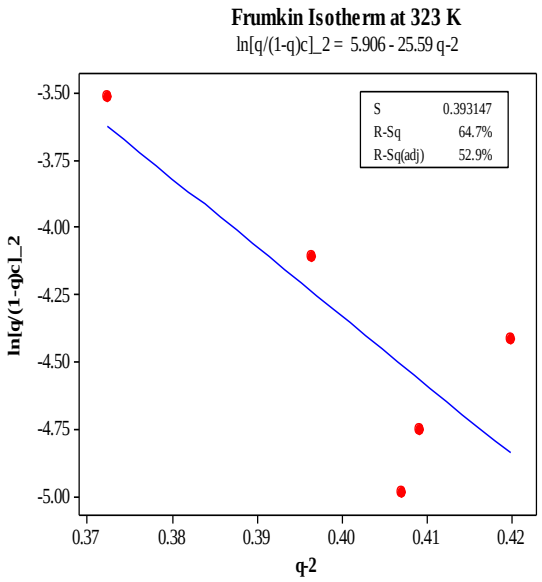
Frumkin Isotherm at 323 K
ln[q/(1-q)c]_2 = 5.906 - 25.59 q-2
S 0.393147
R-Sq 64.7%
R-Sq(adj) 52.9%
ln[q/(1-qc]_2
q-2

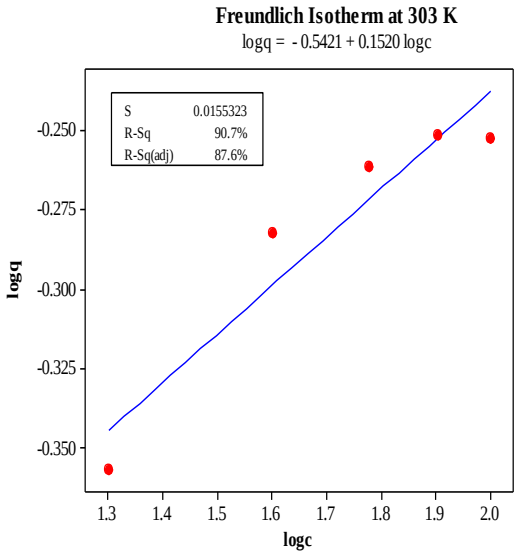
Freundlich Isotherm at 303 K
logq = - 0.5421 + 0.1520 logc
S 0.0155323
R-Sq 90.7%
R-Sq(adj) 87.6%
logq
logc

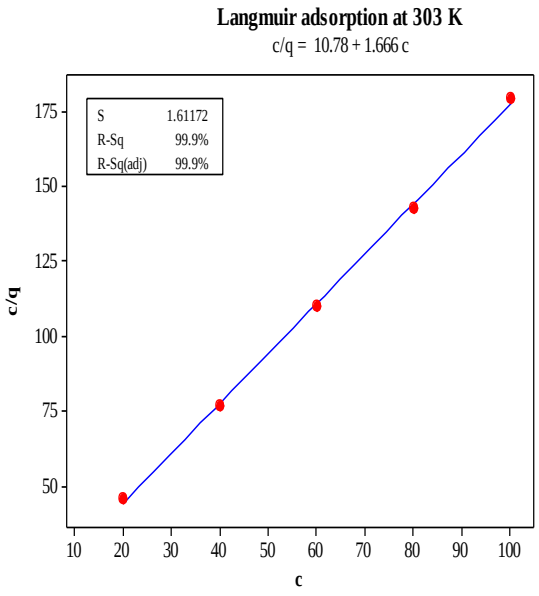
Langmuir adsorption at 303 K
c/q = 10.78 + 1.666 c
S 1.61172
R-Sq 99.9%
R-Sq(adj) 99.9%
c/q
c

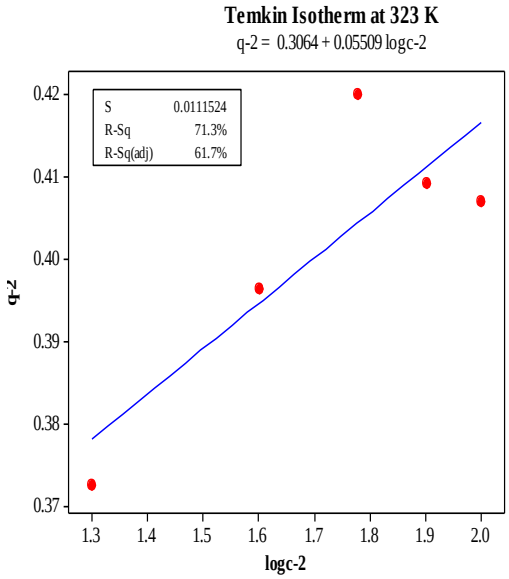
Temkin Isotherm at 323 K
q-2 = 0.3064 + 0.05509 logc-2
S 0.0111524
R-Sq 71.3%
R-Sq(adj) 61.7%
q-2
logc-2

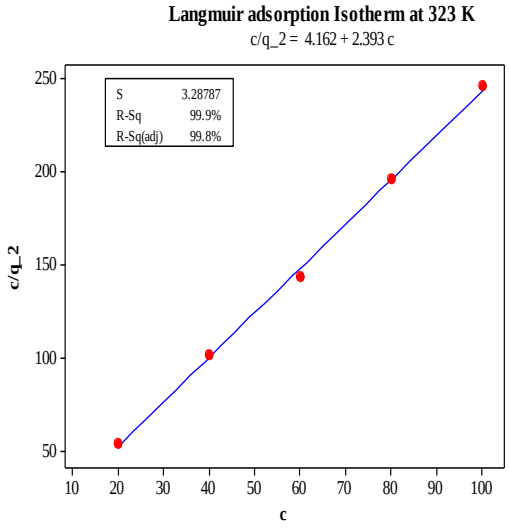
Langmuir adsorption Isotherm at 323 K
c/q_2 = 4.162 + 2.393 c
S 3.28787
R-Sq 99.9%
R-Sq(adj) 99.8%
c/q_2
c
250
200
150
100
50
10
20
30
40
50
60
70
80
90
100

(ii) Activation energies

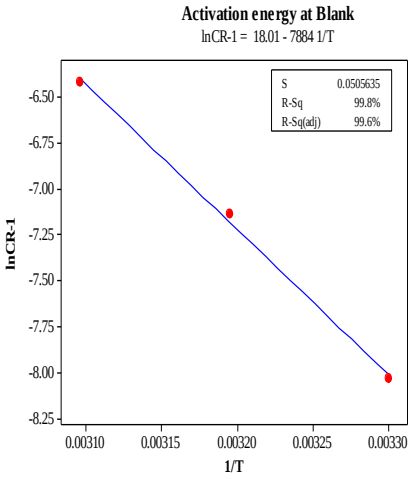

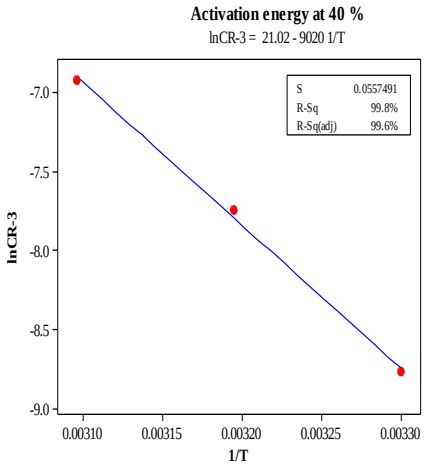

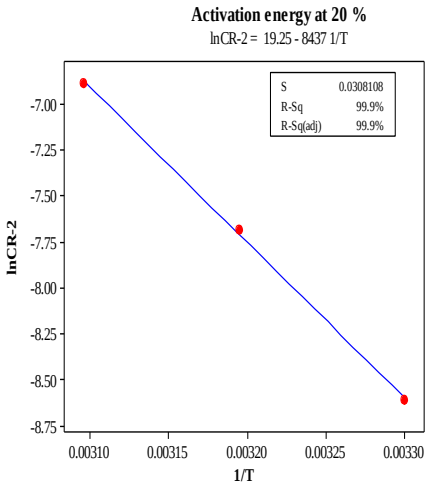

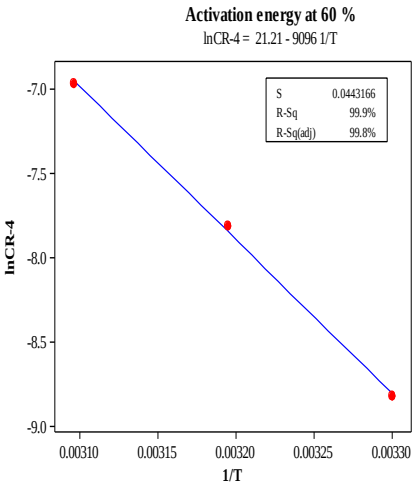

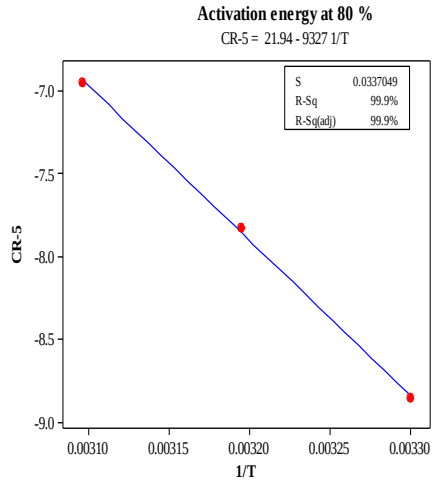

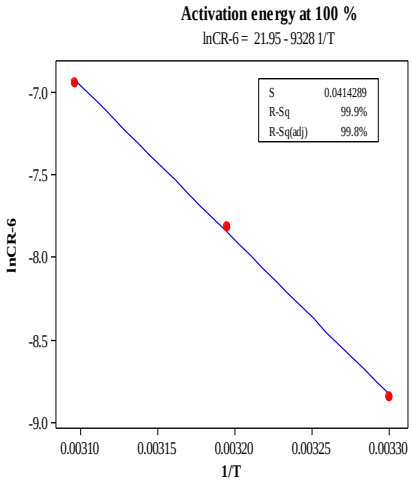

(ii) Enthalapies of activation and entropies

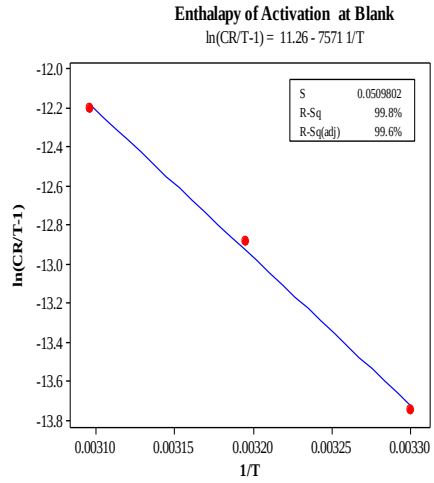

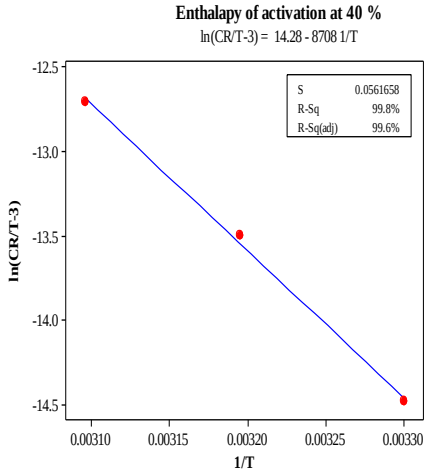

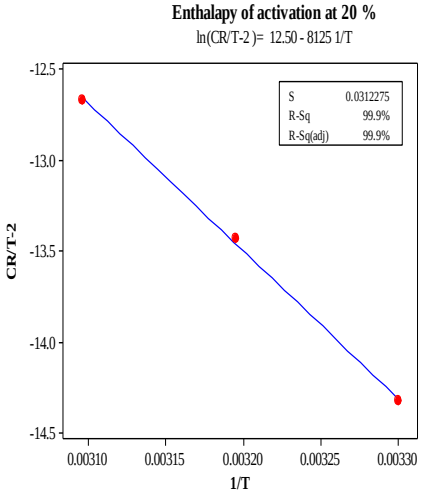
Enthalapy of activation at 20 %
ln(CR/T-2)= 12.50 - 8125 1/T
S 0.0312275
R-Sq 99.9%
R-Sq(adj) 99.9%
CR/T-2
-12.5
-13.0
-13.5
-14.0
-14.5
0.00310
0.00315
0.00320
0.00325
0.00330
1/T

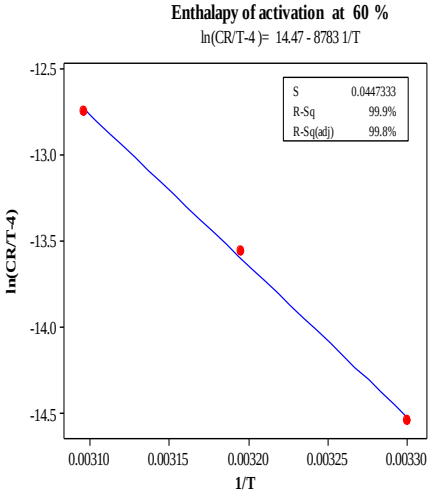
Enthalapy of activation at 60 %
ln(CR/T-4)= 14.47 - 8783 1/T
S 0.0447333
R-Sq 99.9%
R-Sq(adj) 99.8%
ln(CR/T-4)
-12.5
-13.0
-13.5
-14.0
-14.5
0.00310
0.00315
0.00320
0.00325
0.00330
1/T

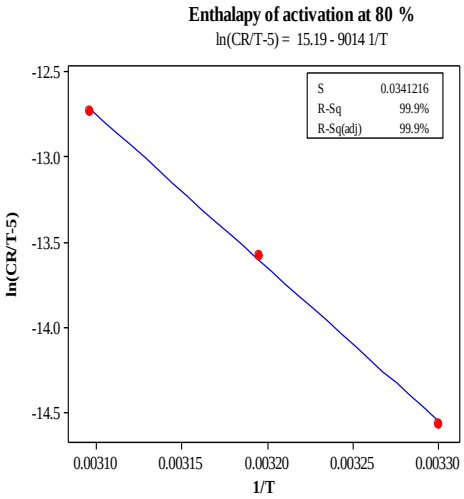
Enthalapy of activation at 80 %
ln(CR/T-5) = 15.19 - 9014 1/T
S 0.0341216
R-Sq 99.9%
R-Sq(adj) 99.9%
ln(CR/T-5)
-12.5
-13.0
-13.5
-14.0
-14.5
0.00310
0.00315
0.00320
0.00325
0.00330
1/T

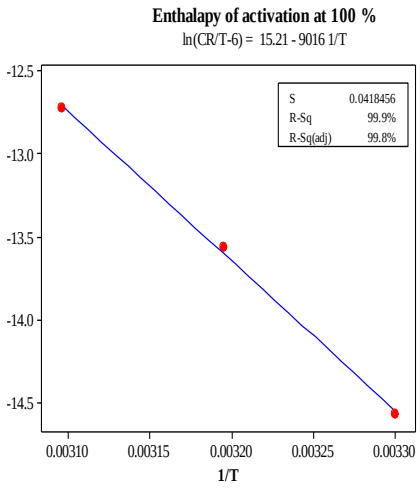
Enthalapy of activation at 100 %
ln(CR/T-6) = 15.21 - 9016 1/T
S 0.0418456
R-Sq 99.9%
R-Sq(adj) 99.8%
-12.5
-13.0
-13.5
-14.0
-14.5
0.00310
0.00315
0.00320
0.00325
0.00330
1/T

(iv) Heats of adsorption

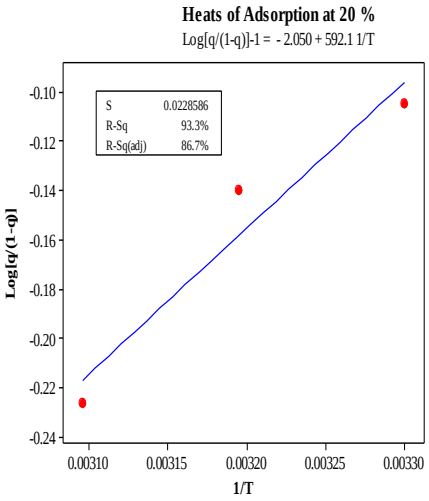

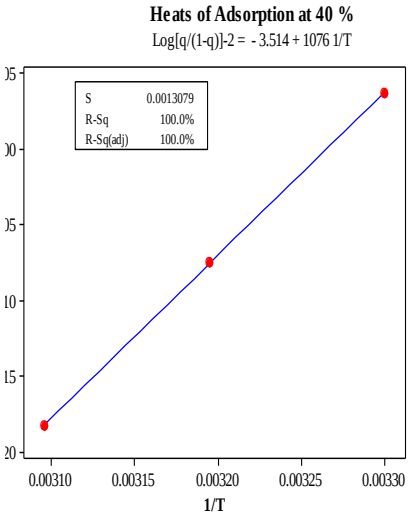

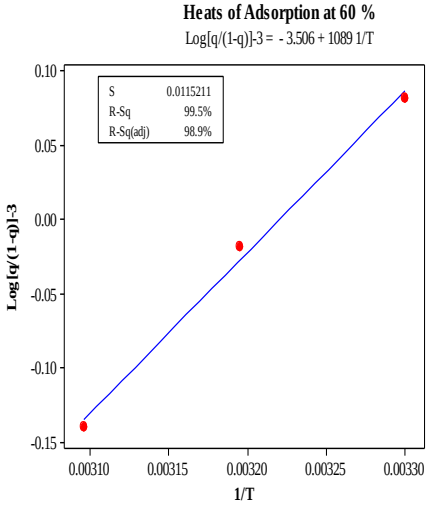

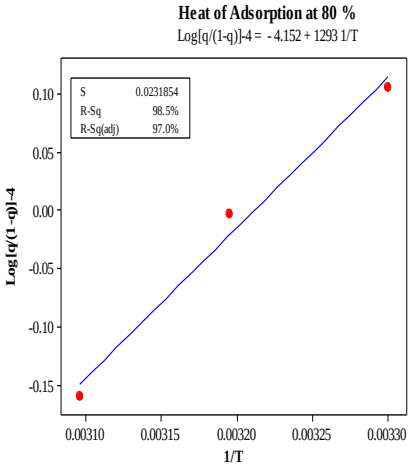

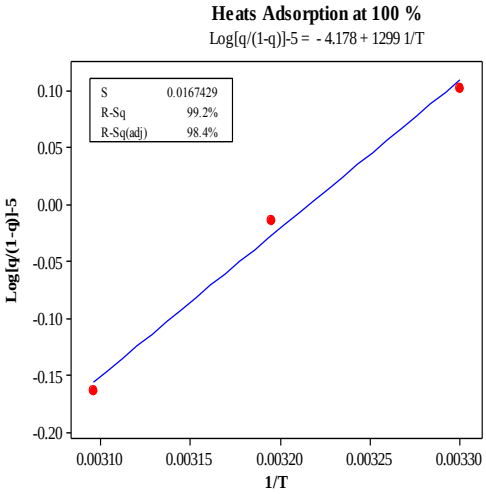
Heats Adsorption at 100 %
Log[q/(1-q)]-5 = - 4.178 + 1299 1/T
S 0.0167429
R-Sq 99.2%
R-Sq(adj) 98.4%
0.10
0.05
0.00
-0.05
-0.10
-0.15
-0.20
Log[q/(1-q)]-5
0.00310
0.00315
0.00320
0.00325
0.00330
1/T